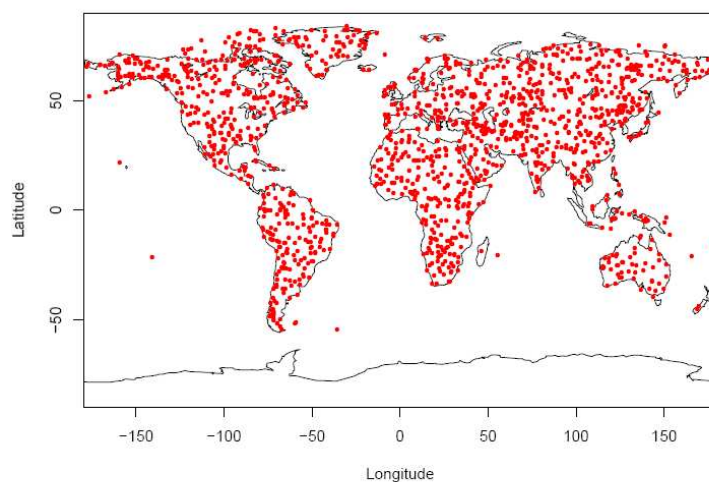




Technical Report No. 39

REFERENCE EVAPOTRANSPIRATION WITH RADIATION-BASED AND TEMPERATURE-BASED METHODS - IMPACT ON HYDROLOGICAL DROUGHT USING WATCH FORCING DATA



Lieke A. Melsen, Henny A.J. van Lanen, Niko Wanders,
Marjolein H.J. van Huijgevoort & Graham P. Weedon

6 September 2011



WATCH is an Integrated Project Funded by the European Commission under the Sixth Framework Programme, Global Change and Ecosystems Thematic Priority Area (contract number: 036946). The WACH project started 01/02/2007 and will continue for 4 years.

Title:	Reference evapotranspiration with radiation-based and temperature-based methods – impact on hydrological drought using WATCH Forcing Data
Authors:	Lieke A. Melsen, Henny A.J. van Lanen, Niko Wanders, Marjolein H.J. van Huijgevoort & Graham P. Weedon
Organisations:	<ul style="list-style-type: none">- Wageningen University - Hydrology and Quantitative Water Management Group (WUR)- Utrecht University – Department of Physical Geography- UK Met Office
Submission date:	6 September 2011
Function:	This report is an output from Work Block 1; Task 1.3.3. Variability of ensemble datasets for the 20th century, and Work Block 4; Task 4.1.1 Investigate processes controlling the propagation of drought.
Deliverable	WATCH deliverables D 1.3.4 Report on the uncertainty of the global water cycle of the 20th Century, D 4.1.4 Report on the increased understanding of the propagation of drought in different hydro-climatological regions, physical catchment structures and different scales, and D 4.1.5 Generic method to quantify the propagation of a drought.

Photo cover: **Left:** Dry streamflow gauging station in the Upper-Guadiana Basin (2008) with a meteorological station at top of the roof
 Right: Global map with location of land points where the radiation-based and the temperature-based methods are intercompared.

Contents

Summary	vi
1 Introduction	1
2 Methods and Materials	3
2.1 WATCH Forcing Data	3
2.2 Penman-Monteith reference evapotranspiration	5
2.2.1 Radiation-based Penman-Monteith method	8
2.2.2 Temperature-based Penman-Monteith method	8
2.3 Hydrological Model	10
2.4 Defining Droughts	13
3 Results	15
3.1 Overview all climates	15
3.1.1 Evapotranspiration	15
3.1.2 Hydrological Drought	21
3.2 Equatorial A Climates	22
3.2.1 Evapotranspiration	22
3.2.2 Hydrological Drought	23
3.3 Arid B Climates	23
3.3.1 Evapotranspiration	24
3.3.2 Hydrological Drought	25
3.4 Warm temperate C Climates	26
3.4.1 Evapotranspiration	26
3.4.2 Hydrological Drought	27
3.5 Snow D Climates	28
3.5.1 Evapotranspiration	28
3.5.2 Hydrological Drought	29
3.6 Polar E Climates	29
3.6.1 Evapotranspiration	30
3.6.2 Hydrological Drought	31
4 Concluding remarks	33
References	34
Appendices	36
A Climate A	I
A.1 Reference evapotranspiration ET_0	I
A.2 Actual evapotranspiration ET_A	II
A.3 Hydrological drought characteristics	IV
B Climate B	V
B.1 Reference evapotranspiration ET_0	V
B.2 Actual evapotranspiration ET_A	VI
B.3 Hydrological drought characteristics	IX
C Climate C	X
C.1 Reference evapotranspiration ET_0	X
C.2 Actual evapotranspiration ET_A	XI
C.3 Hydrological drought characteristics	XIII

D Climate D	XIV
D.1 Reference evapotranspiration ET_0	XIV
D.2 Actual evapotranspiration ET_A	XV
D.3 Hydrological drought characteristics	XVII
E Climate E	XVIII
E.1 Reference evapotranspiration ET_0	XVIII
E.2 Actual evapotranspiration ET_A	XIX
E.3 Hydrological drought characteristics	XXI
F Overview	XXII
F.1 Evapotranspiration ET	XXII
F.2 Hydrological drought characteristics	XXIV

Summary

In this report, two different methods to calculate reference evapotranspiration are applied and compared. This has been done in response to inconsistencies among the daily variables in the WATCH Forcing Data (WFD). One method is so-called radiation based (ET_{0rad}), and is the well known Penman-Monteith equation with, among others, incoming short wave radiation as a variable. The radiation-based method used the variables T_{air} , T_{max} and T_{min} , $Wind$, SW_{down} , LW_{net} , Q_{air} and P_{Surf} from the WFD. The other method is so-called temperature-based (ET_{0temp}), the radiation term is replaced by an approximation of the radiation based on minimum and maximum air temperature. The temperature-based method only used the variables T_{air} , T_{max} , T_{min} and $Wind$ from the WFD. After calculating reference evapotranspiration ET_0 with both methods, it is fed into a conceptual hydrological model that combines a soil water balance and a simple lumped groundwater model. The model generates a daily water balance, e.g. potential evapotranspiration (ET_P), actual evapotranspiration (ET_A), soil moisture storage, groundwater recharge and groundwater discharge. Eventually, the simulated groundwater discharge is used to define periods of drought with a Variable Threshold (VT) method. The VT in this study used Q_{80} , implying that a period is designated as drought as soon as the groundwater discharge is in the lowest 20% of all simulated discharges for that particular month. Drought periods and characteristics, like length and deficit, are identified. The model using the two different ET_0 series, is applied to 1495 cells (land grids) that well represent the five Köppen-Geiger major climates across the world.

First, a comparison is made between the ET_{0rad} and ET_{0temp} . There are clearly differences between the two methods, and generally the radiation-based method leads to higher ET_0 than the temperature-based method. There are some exceptions within the different major climates, and also the northern and the southern hemisphere behave differently in this perspective. The differences between ET_{Arad} and ET_{Atemp} are significantly smaller than for the reference evapotranspiration. In general the radiation-based method still leads to higher ET_A than the temperature-based method, but the difference is smaller and in many cases the difference even decreases to zero (26% of the cells globally). Finally, the different drought characteristics are compared. There are remarkable differences in drought characteristics, especially in deficit volume and intensity, but in general the differences are within ranges found in other literature that describes the impact of hydrological models or datasets with different diurnal forces on hydrological drought. Climate D and E, the snow-affected climates, show the largest differences.

1 Introduction

More emphasis is put on drought research over the last years, because of the rising water demands worldwide (Tallaksen and Van Lanen, 2004; WWDR, 2009) and the expected climate changes, where a dryer and warmer Mediterranean region and a shift of climatic regimes in Europe northward is expected (IPCC, 2007). A generally accepted definition of drought is proposed by Wilhite (2000) and Tallaksen and Van Lanen (2004):

A sustained and regional extensive occurrence of below average natural water availability.

This definition makes clear that drought is a quantity which can not be measured directly, but can be characterized by multiple climatological and hydrological indicators (Wilhite, 2000; Tallaksen and Van Lanen, 2004; Mishra and Singh, 2010). Hydrological drought starts with a meteorological drought (Changnon, 1989). Lack of precipitation and high evapotranspiration signals propagate from a meteorological drought to an agricultural (soil moisture) drought and eventually to a hydrological drought with lower groundwater recharge, storage and discharge. Evapotranspiration is thus an important variable in determining hydrological drought.

Problem context

Within the European funded project WATER and global CHange (WATCH, www.eu-watch.org) a global sub-daily meteorological data set is generated, the WATCH Forcing Data (WFD) (Weedon *et al.*, 2011). With the WFD, reference evapotranspiration ET_0 can be calculated. Subsequently, potential (ET_P) and actual evapotranspiration (ET_A) and the influence on groundwater discharge can be modeled using this reference evapotranspiration. The WFD were derived from a reanalysis of the ERA-40 data (Uppala *et al.*, 2005). Unfortunately, there seems to be some inconsistency between the daily radiation and temperature data due to an independent correction of the meteorological data. The radiation term is requisite input for the Penman-Monteith equation to calculate reference evapotranspiration (Allen *et al.*, 1998). However, it is possible to replace the radiation term in the Penman-Monteith equation by approximations based on, among others, minimum (T_{min}) and maximum (T_{max}) temperature (Allen *et al.*, 1998), meaning that it changes from a so-called radiation-based method to a temperature-based method.

Objective and Research questions

The objective of this study is to describe the difference between the reference evapotranspiration ET_0 calculated with a radiation-based method and with a temperature-based method and its impact on drought characteristics across the world.

This leads to the following research questions:

- What is the difference between the reference evapotranspiration calculated with the radiation-based method and the reference evapotranspiration calculated with a temperature-based method?
- What is the effect in different climatic regions as defined by the Köppen-Geiger classification?
- What is the influence of the difference in reference evapotranspiration on hydrological drought across the world?

Method

The Köppen-Geiger climate classification (Kottek *et al.*, 2006; Wanders *et al.*, 2010) will be used to study the spatially distributed impact of reference evapotranspiration on hydrological drought across the world. For the calculation of the reference evapotranspiration, the Penman-Monteith equation as proposed by the FAO (Allen *et al.*, 1998) will be used. Daily meteorological input for this equation will be retrieved from the WFD. The method will be used to calculate the reference evapotranspiration with and without the radiation term as proposed by Allen *et al.* (1998). Based on the climate classification of Köppen-Geiger as defined by Kottek *et al.* (2006) and recalculated with the WFD by Wanders *et al.* (2010), WFD cells are stratified-randomly selected in the 31 different sub climates. For all selected cells of every sub climate an analysis is done to determine the difference between the two reference evapotranspiration series. With a hydrological model, actual evapotranspiration and discharge will be simulated, the propagation of drought in the hydrological cycle (delay, attenuation,

lengthening, Van Lanen *et al.*, 2011). With drought characteristics like deficit volume and duration an analysis of the period 1958-2001 will be done.

Outline

First the WATCH Forcing Data (WFD) are introduced in Chapter 2. The WFD are used to calculate reference evapotranspiration with two different methods. These two methods will also be explained in Chapter 2, as well as the hydrological model that is used to simulate a water balance with the use of ET_0 and the WFD. Chapter 2 will end with an explanation how drought periods are identified and which characteristics are determined to compare drought all over the globe.

In Chapter 3 the results from all the data processing are presented. First in general for all climates, and then per major climate. Per climatic region the reference evapotranspiration ET_0 , actual evapotranspiration ET_A and drought characteristics will be discussed. Some more details from sub climates within the major climate are presented.

Chapter 4 contains the concluding remarks from the comparison between the two different methods, discussed for ET_0 , ET_A and drought characteristics.

2 Methods and Materials

This chapter describes the methods and data used to calculate the reference evapotranspiration and the hydrological model used to determine actual evapotranspiration and discharge. First an overview of the WATCH Forcing Data (WFD) is provided. Thereafter, one can find descriptions of the methods used to obtain reference evapotranspiration. Then a description of the hydrological model that is used to simulate the actual evapotranspiration, groundwater recharge and discharge is given. Finally, the method is described to identify drought characteristics.

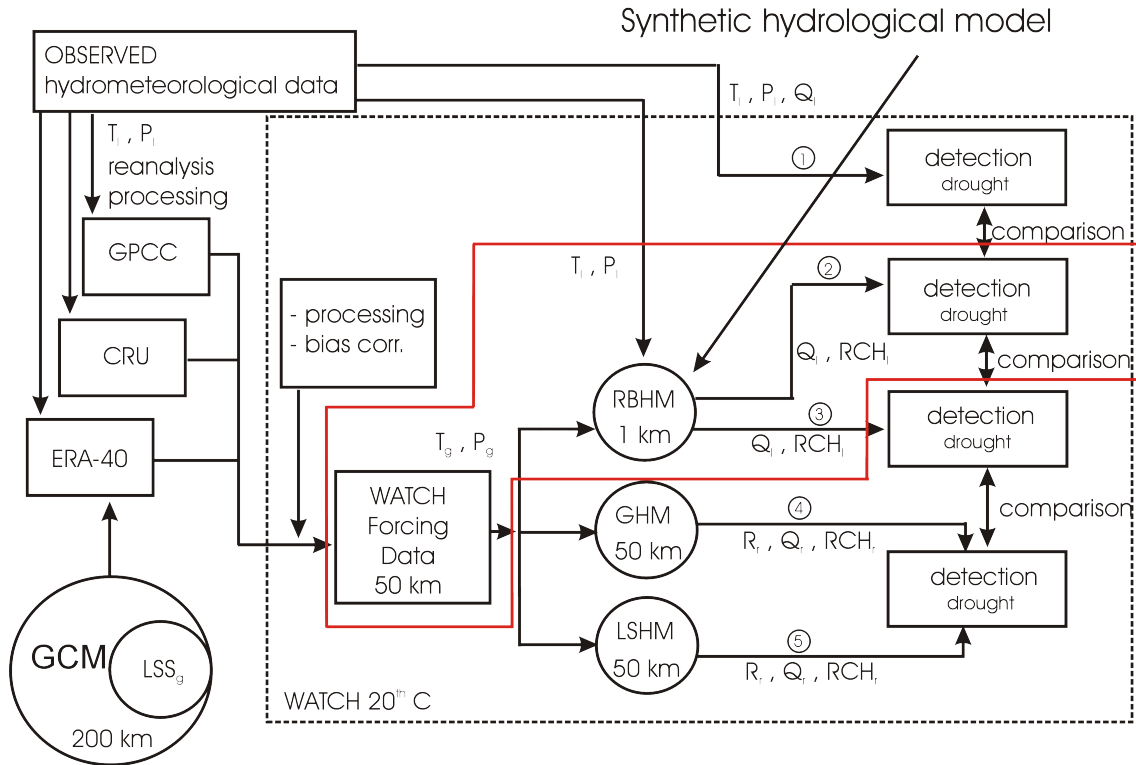


Figure 1: Flow chart showing the context of the intercomparison of the two methods to calculate the reference evapotranspiration within WATCH.

Figure 1 shows how the two different methods to calculate the reference evapotranspiration fit with the overall WATCH research. The WATCH Forcing Data (WFD, Section 2.1) offer the opportunity to compute reference evapotranspiration in different ways. These different series of reference evapotranspiration data are used as input for a hydrological model (i.e. synthetic model, Section 2.3) to explore the influence on hydrological drought characteristics (i.e. detection of extremes). The outcome helps to assess the uncertainty caused by the WFD, but also contributes to the understanding of differences in drought characteristics simulated with global hydrological models (GHMs) and land surface models (LSMs), which use different concepts for the calculation of the reference evapotranspiration.

2.1 WATCH Forcing Data

The WATCH Forcing Data (WFD) is a data set that contains data of eleven different meteorological variables over the period 1958 - 2001¹ at a half degree resolution, at 67.420 different land points following the CRU land mask. The WFD have been derived from the reanalysis product of the ERA-40 dataset (Uppala *et al.*, 2005), from the European Centre for Medium Range Weather Forecasting (ECMWF), the CRU TS2.1 dataset (Mitchell and Jones, 2005), and the GPCCR full data product (Schneider *et al.*, 2008). Table 1 gives an overview of all the data sources for the WFD. A brief

¹First phase: 1958-2001. In the second phase the dataset has been extended to cover the whole 20th century (1901-2001). In this study only data from 1958-2001 are used

Table 1: Data sources for WATCH Forcing Data (adapted from Weedon *et al.*, 2011)

Dataset	Summary
ERA-40	ECMWF reanalysis product
CRU TS2.1	Climate Research Unit gridded station based observations (multiple variables)
GPCC Full data product v4	Global Precipitation Climatology Centre gridded station based precipitation observations

Table 2: Description of variables in WATCH Forcing Data (adapted from Weedon *et al.*, 2011)

ALMA variable	Variable description	Units	Time step
T_{air}	2 m air temperature (instantaneous)	K	6 hourly
$PSurf$	10 m surface pressure (instantaneous)	Pa	6 hourly
Q_{air}	2 m specific humidity (instantaneous)	kg/kg	6 hourly
U_{10}	10 m speed (instantaneous)	m/s	6 hourly
LW_{down}	Downwards long-wave radiation flux (average)	W/m^2	6 hourly
LW_{net}	Net short-wave radiation flux (average)	W/m^2	6 hourly
SW_{down}	Downwards short-wave radiation flux (average)	W/m^2	3 hourly
$Rainf$	Rainfall rate GPCC bias and undercatch-corrected (average)	$kg/m^2/s$	3 hourly
$Snowf$	Snowfall rate GPCC bias and undercatch-corrected (average)	$kg/m^2/s$	3 hourly
$Rainf$	Rainfall rate CRU bias and undercatch-corrected (average)	$kg/m^2/s$	3 hourly
$Snowf$	Snowfall rate CRU bias and undercatch-corrected (average)	$kg/m^2/s$	3 hourly

description of all the variables in the WFD is given in Table 2. Next to these sub daily data, daily averaged data from all the variables are available. There are also some additional files containing daily values for T_{min} and T_{max} based on the 3-hourly data.

The CRU data are available at a spatial resolution of $0.5^\circ \times 0.5^\circ$, whereas the ERA-40 have a spatial resolution of $1.0^\circ \times 1.0^\circ$. Before the bias-correction was applied, the ERA-40 data is interpolated to the CRU grid. This downscaling in spatial resolution led to some potential inconsistencies with the elevation. Therefore an elevation correction to account for differences in surface height was necessary for certain variables (temperature, surface pressure, specific humidity and downwards long-wave radiation flux). The ERA-40 data set does not agree on temperature with the CRU observations. The monthly T_{air} is adjusted to the CRU average temperatures. The corrections for LW_{down} at each time step include the adjusted temperature values and the adjusted pressure and specific humidity values. So the monthly offsets in T_{air} are incorporated into monthly average LW_{down} through the elevation correction. However, at the daily time scale an inconsistency due to the monthly T_{air} corrections could feed through into the difference between LW_{down} and LW_{up} . SW_{down} has also been adjusted to be consistent with CRU cloud cover fraction and the effects of variations in atmospheric aerosol loading. Potentially this implies further inconsistency between SW_{net} and LW_{net} . For an overview of all the corrections, see Weedon *et al.* (2011).

WATCH Forcing Data used in this study

For the calculations done in this study, daily averages of the WFD are used. These averages are calculated from 3 hourly simulations as the arithmetic mean. The daily averaged values are directly available in the WFD.

In this study a stratified random sample of locations in the WATCH Forcing Dataset is taken (Wanders *et al.*, 2010; Van Lanen *et al.*, 2011). To make sure that all different climates are represented in the

Table 3: Indicators for different climates (derived from Kottek *et al.*, 2006)

Main Climates	Precipitation	Temperature
A: equatorial	W: desert	h: hot arid
B: arid	S: steppe	k: cold arid
C: warm temperate	f: fully humid	a: hot summer
D: snow	s: summer dry	b: warm summer
E: polar	w: winter dry	c: cool summer
	m: monsoonal	d: extremely continental
		F: polar frost
		T: polar tundra

selected locations, a random selection was processed per climatic region (stratified sample) as defined by Kottek *et al.* (2006) and Wanders *et al.* (2010) based on the Köppen-Geiger climate classification. This classification distinguishes 31 different climates, that are labelled with three letters: a main climate, a precipitation indicator, and a temperature indicator (see Table 3), and determined with different climatic parameters, see Table 4. In every climate, 2% of the cells were randomly selected, with a minimum of 20 cells. It appears that in some climatic regions less than 20 cells were available, e.g. in the Csc climate, which in that case were all selected. Table 5 gives the number of cells selected per major climate (column 3), and per sub climate (column 8). The criteria for climate Dsd are not met with the WFD, so the selected locations are distributed over 30 different climates. For Dsd zero cells are selected. In total, 1495 locations from the 67.420 cells were selected (2.2%) from over the whole earth. A bootstrap analysis showed that this selection is sufficient to cover the 90% probability fields of the combined drought duration and standardized deficit volume (Van Lanen *et al.*, 2011). Figure 2 gives an overview of how the locations are distributed over the world. Note that the selected cells are not equally distributed over the northern and southern hemisphere: 80.5% of all the cells are in the northern hemisphere.

Table 4: Climatic parameters to determine climatic regions (adapted from Kottek *et al.*, 2006)

Symbol	Description
P_{min}	Minimum monthly precipitation
P_{ann}	Mean annual precipitation
P_{smin}	Minimum summer precipitation
P_{wmin}	Minimum winter precipitation
P_{smax}	Maximum summer precipitation
P_{wmax}	Maximum winter precipitation
P_{th}	Dryness threshold
T_{Mmin}	Minimum monthly temperature
T_{Mmax}	Maximum monthly temperature
T_{mon}	Monthly temperature

2.2 Penman-Monteith reference evapotranspiration

The method described in this section will be applied to obtain reference evapotranspiration ET_0 from the WFD. Further details are given by Allen *et al.* (1998).

Evapotranspiration is often one of the hardest terms in the water balance to determine. In 1948, Penman combined the energy balance and the mass transfer method and proposed a formula to calculate evaporation from an open water surface. In 1965, this formula has been reformulated by Monteith, to make it applicable to dry, horizontal, vegetated surface with optimal water supply (Monteith, 1965). The reference crop that is assumed to be representative for ET_0 has the following definition, as defined by the FAO Expert Consultation on Revision of FAO Methodologies for Crop Water Requirements (Allen *et al.*, 1998):

Table 5: Number of cells selected per (sub)climate (adapted from Van Lanen *et al.*, 2011)

Major	Description	Nr.	Climate	Subtype	Code	Description	Nr.		
A	Equatorial	235	Af	rainforest		fully humid	54		
			Am	monsoon			38		
			As	savannah		dry summer	20		
			Aw			dry winter	123		
B	Arid	313	BW	desert	BWk	cold	37		
					BWh	hot	147		
			BS	steppe	BSk	cold	66		
					BSh	hot	63		
C	Warm Temperate	242	Cf	fully humid	Cfa	hot summer	60		
					Cfb	warm summer	48		
					Cfc	cool summer	20		
						cold winter			
					Cs	dry summer	Csa	hot summer	23
							Csb	warm summer	20
			Csc	cool summer			11		
			Cw	dry winter	Cwa	hot summer	30		
					Cwb	warm summer	20		
					Cwc	cool summer	10		
						cold winter			
					D	Snow	506	Df	fully humid
Dfb	warm summer	90							
Dfc	cool summer	222							
	cold winter								
Dfd	extremely con- tinental	28							
Ds	dry summer	Dsa	hot summer	20					
		Dsb	warm summer	20					
		Dsc	cool summer	20					
			cold winter						
		Dsd	extremely con- tinental	0					
		Dw	dry winter	Dwa				hot summer	20
Dwb	warm summer			20					
Dwc	cool summer			26					
	cold winter								
Dwd	extremely con- tinental			20					
E	Polar			199	EF	frost			40
		ET	tundra				159		

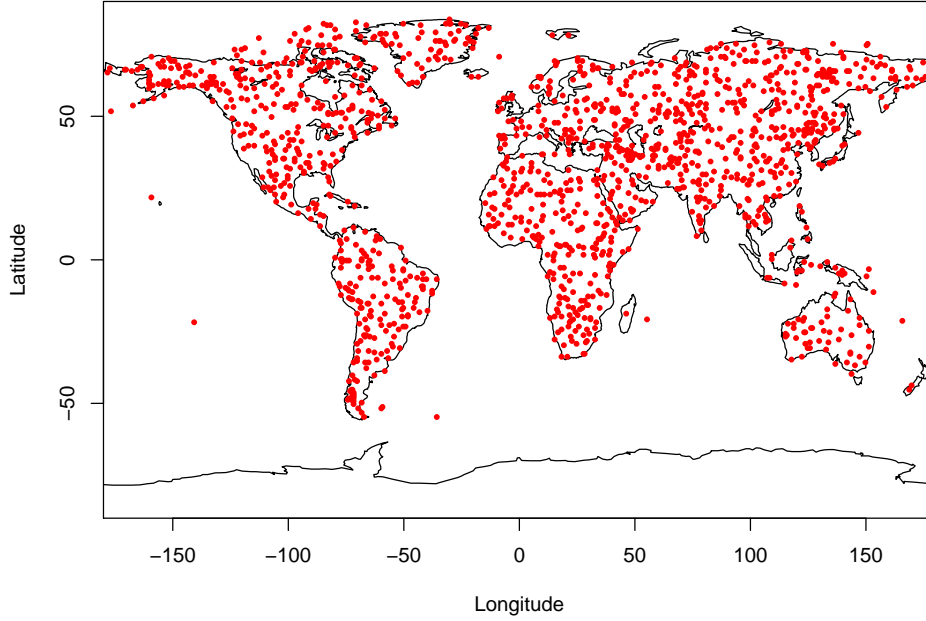


Figure 2: Distribution of the selected locations from the WFD.

A hypothetical reference crop with an assumed crop height of 0.12 meter, a fixed surface resistance of 70 sm^{-1} and an albedo of 0.23.

The Penman-Monteith equation computes the potential evapotranspiration ET_P for this reference crop, which is also called the reference evapotranspiration ET_0 , with the following equation:

$$ET_0 = \frac{0.408\Delta(R_n - G) + \gamma \frac{900}{T_{air} + 273.15} u_2 (e_s - e_a)}{\Delta + \gamma(1 + 0.34u_2)} \quad (1)$$

Where:

ET_0 = reference evapotranspiration	(mm/day)
R_n = net radiation	(MJ/m ² /day)
G = soil heat flux	(MJ/m ² /day)
$(e_s - e_a)$ = vapor pressure deficit of the air	(kPa)
T_{air} = mean daily air temperature at 2 m	(°C)
u_2 = wind speed at 2 m height	(m/s)
Δ = slope of saturation vapor pressure curve	(kPa/°C)
γ = psychrometric constant = 0.067	(kPa/°C)

The soil heat flux G is set to 0, which is a good approximation averaged over a day. The mean daily temperature T_{air} is directly available in the WFD (Section 2.1). The 2 m wind speed u_2 is converted from the 10 m ($z=10$) wind speed which is available in the WFD via the following equation:

$$u_2 = \frac{u_z * 4.87}{\log(67.8 * z - 5.42)} \quad (2)$$

The slope of the saturation pressure is calculated with:

$$\Delta = 4098 * \frac{0.6108 * e^{17.27 \frac{T_{air}}{T_{air} + 237.3}}}{(T_{air} + 237.3)^2} \quad (3)$$

where for T_{air} the daily average from the WFD is used.

The only terms that still have to be described are R_n , the net radiation, and $(e_s - e_a)$, the vapor pressure deficit of the air. The net radiation can be calculated with the following equation:

$$R_n = SW_{net} + LW_{net} \quad (4)$$

The net shortwave radiation can be obtained with the albedo α , which is 0.23 for the reference crop:

$$SW_{net} = 1 - \alpha * SW_{down} \quad (5)$$

The net longwave radiation and the shortwave downwards radiation are obtained differently for the temperature-based and the radiation-based method. The calculation for the vapor pressure deficit is also different for both methods. The equations for SW_{down} and $e_s - e_a$ used in this study can be found in the following subsections.

2.2.1 Radiation-based Penman-Monteith method

For the radiation-based method SW_{down} and LW_{net} are used to estimate reference evapotranspiration. The net radiation LW_{net} and the SW_{down} are both directly available in the WFD (Section 2.1). The vapor pressure deficit of the air is calculated with:

$$e^0(t) = 0.6108 * e^{\frac{17.27T}{T+237.3}} \quad (6)$$

$$e_s = \frac{e_{Tmax}^0 + e_{Tmin}^0}{2} \quad (7)$$

$$e_a = \frac{Q_{air} * P_{Surf}}{\varepsilon} \quad (8)$$

Where for e_{Tmax}^0 $T = T_{max}$ is used, and for e_{Tmin}^0 $T = T_{min}$. To calculate e_a (Stull, 2000), Q_{air} and P_{Surf} are available in the WFD (Section 2.1). ε is 0.622, the ratio of the gas constant for dry air and water vapor.

2.2.2 Temperature-based Penman-Monteith method

An alternative to compute ET_0 with Penman-Monteith without radiation data, is to approach the radiation-term SW_{down} and LW_{net} by, among others, minimum and maximum temperature. In this study this so-called temperature-based method is applied because there might be mutual inconsistencies in the radiation and temperature data (Section 2.1). The temperature-based method is further described in Allen *et al.* (1998).

The short wave radiation that reaches the earth is estimated with the temperature difference between T_{min} and T_{max} :

$$SW_{down} = k_{SW_{down}} * \sqrt{T_{max} - T_{min}} * R_a \quad (9)$$

where:

$$\begin{aligned} SW_{down} &= \text{downwards shortwave radiation} && (MJ/m^2/day) \\ k_{SW_{down}} &= \text{adjustment coefficient} && (^\circ C^{-0.5}) \\ R_a &= \text{extraterrestrial radiation} && (MJ/m^2/day) \\ T_{max} &= \text{maximum air temperature} && (^\circ C) \\ T_{min} &= \text{minimum air temperature} && (^\circ C) \end{aligned}$$

T_{max} and T_{min} are available in additional WFD files, for which the highest and lowest measurement of eight daily temperature measurements were used. The adjustment coefficient $k_{SW_{down}}$ is 0.16 on

land-mass dominated locations, and 0.19 on water-influenced locations (Allen *et al.*, 1998). In this case, the $k_{SW_{down}}$ is kept constant at 0.16, because all points in the WFD are on land, and no clear definition is stated to define influence from water on land. R_a , the extraterrestrial radiation, can be calculated with:

$$R_a = \frac{24(6)}{\pi} * G_{sc} * d_r * [\omega_s \sin(\varphi) \sin(\delta) + \cos(\varphi) \cos(\delta) \sin(\omega_s)] \quad (10)$$

where:

R_a = extraterrestrial radiation	(MJ/m ² /day)
G_{sc} = solar constant = 0.0829	(MJ/m ² /min)
d_r = inverse relative distance Earth-Sun	(-)
ω_s = sunset hour angle	(rad)
φ = latitude	(rad)
δ = solar declination	(rad)

d_r and δ both depend on J , the number of the day in the year (1-365 or 366). ω_s depends again on δ and φ , the solar declination and latitude respectively. The equations can be found below:

$$d_r = 1 + 0.33 * \cos\left(\frac{2\pi}{365} J\right) \quad (11)$$

$$\delta = 0.409 * \sin\left(\frac{2\pi}{365} J - 1.39\right) \quad (12)$$

$$\omega_s = \arccos[-\tan(\varphi)\tan(\delta)] \quad (13)$$

R_a can be inserted in in equation 9. With the known SW_{down} , the net longwave radiation can be calculated:

$$LW_{net} = \sigma \left[\frac{T_{max,K}^4 + T_{min,K}^4}{2} \right] (0.34 - 0.14\sqrt{e_a}) \left(1.35 \frac{SW_{down}}{R_{s0}} - 0.35 \right) \quad (14)$$

LW_{net} = net longwave radiation	(MJ/m ² /day)
SW_{down} = downwards shortwave radiation	(MJ/m ² /day)
α = albedo = 0.23	(-)
σ = Stefan-Boltzmann constant = $4.903 * 10^{-9}$	(MJ/K ⁴ /m ² /day)
$T_{max,K}$ = max absolute temperature	(K)
$T_{min,K}$ = min absolute temperature	(K)
e_a = actual vapor pressure	(kPa)
R_{s0} = clear-sky radiation	(MJ/m ²)

$T_{min,K}$ and $T_{max,K}$ are available in the additional files of the WFD, containing daily T_{max} and T_{min} .

R_{s0} is given by:

$$R_{s0} = (a_s + b_s) * R_a \quad (15)$$

Where $a_s + b_s$ is the fraction of extraterrestrial radiation that is reaching the earth on days with a clear sky. In this study no explicit values for $a_s + b_s$ were available. Assumed is $a_s = 0.75$ and $b_s = 2 * 10^{-5} * z$ (Allen *et al.*, 1998), where z is the elevation above sea level. e_a is given by

$$e_a = 0.6180 * e^{\frac{17.27 * T_{dew}}{T_{dew} + 237.3}} \quad (16)$$

T_{dew} is the dew point temperature. This temperature was not available in the WFD, and is therefore replaced by T_{min} as proposed by Allen *et al.* (1998) to calculate e_a .

The vapor pressure deficit of the air for the temperature-based method is calculated with equation 6 and 7, like for the radiation-based method. For e_a , equation 16 is used. This is different from the radiation-based method because for the temperature-based method Q_{air} is not used, to prevent using any data that might be inconsistent with other variables. However, the method used for the radiation-based method is in general more exact because for equation 16 the dew point temperature is estimated with the minimum temperature.

The temperature-based method is not applicable in regions where the sun does not rise, for example in the north during winter. There is no direct sunlight which will lead to an unrealistic value for R_a . In these areas during these circumstances the ET_0 , and subsequently ET_A are set to zero.

2.3 Hydrological Model

After obtaining the ET_0 with both the radiation-based and temperature-based method for the 1495 locations over the years 1958-2001, time series of daily groundwater recharge and discharge are simulated by using the NUT_DAY model (Van Lanen *et al.*, 1996). Because the aim of this modeling experiment is purely to explore the forcing effect of the different ET_0 methods, crop type and soil type are kept constant for every selected location on earth. Assumed is that every location has a light silty loam soil (Wösten *et al.*, 2001) and the same crop type, with crop factor $K_c = 1$, e.g. grass. With this crop factor, ET_P can be calculated:

$$ET_P = K_c * ET_0 \quad (17)$$

For $K_c = 1$ this implicates that at every location ET_P is equal to ET_0 (Section 2.2). As mentioned earlier, the temperature-based method is not applicable at certain times of the year at locations where there is no direct sun light, for example in the north during winter. At these locations, ET_P is directly set to zero. Next to that, ET_P is set to zero when the air temperature is below 0°C and a snow cover occurs. ET_P is necessary to calculate ET_A , which in turn determines soil storage.

The NUT_DAY model is developed by Van Lanen *et al.* (1996). It distinguishes two different reservoirs (Figure 3) to compute a water balance of the root zone, generating time series of snow accumulation, soil moisture content, actual evapotranspiration and recharge. In addition it has one reservoir to represent the groundwater system. The NUT_DAY model uses the following balance equations with $\Delta t=1$ day:

$$S_{sn}(t) = S_{sn}(t - \Delta t) + (P_{sn}(t) - Q_{sm}(t))\Delta t \quad (18)$$

$$SS(t) = SS(t - \Delta t) + (P_{ra}(t) + Q_{sm}(t) - ET_a(t) - Rch(t))\Delta t \quad (19)$$

$$S(t) = S(t - \Delta t) - (Q_{out}(t) + Rch(t))\Delta t \quad (20)$$

Where:

S_{sn}	= snow pack storage	(mm)
SS	= soil storage	(mm)
S	= groundwater storage	(mm)
P_{sn}	= snow fall	(mm/day)
P_{ra}	= rainfall	(mm/day)
Q_{sm}	= snow melt rate	(mm/day)
Q_{out}	= groundwater discharge	(mm/day)
ET_a	= actual evapotranspiration	(mm/day)
Rch	= recharge from soil to groundwater	(mm/day)

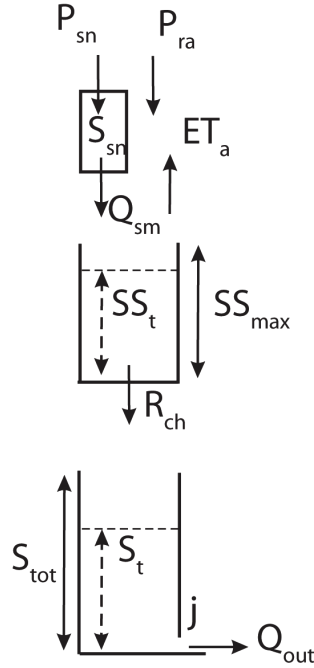


Figure 3: Overview of the different reservoirs within the NUT_DAY model (Wanders *et al.*, 2010).

Snow pack reservoir

In the snow pack reservoir, snow is stored until it melts and drains with a rate Q_{sm} to the soil reservoir with storage SS . For the snow pack reservoir the HBV snow routine (Seibert, 2005) is used. This routine determines based on the temperature whether precipitation will be rain or snow. The separate WFD for snow and rainfall are totalized and then redistributed based on the HBV snow routine. If the precipitation is snow or if there is accumulated snow, this routine also describes the snow melt which starts above a certain threshold temperature TT with a degree-day factor $CFMAX$. Table 6 gives an overview of the snow parameters used as input for the snow reservoir with storage S_{sn} .

Table 6: Snow parameters as used in the NUT_DAY model for this study (Seibert, 2005)

Parameter	Description	Threshold value	
$CFMAX$	degree-day factor	3.5	$mm/^\circ C/day$
CFR	refreezing coefficient	0.05	-
TT	threshold temperature	0.0	$^\circ C$
CWH	water holding capacity	0.1	-
$SFCF$	snow fall correction factor	0.8	-

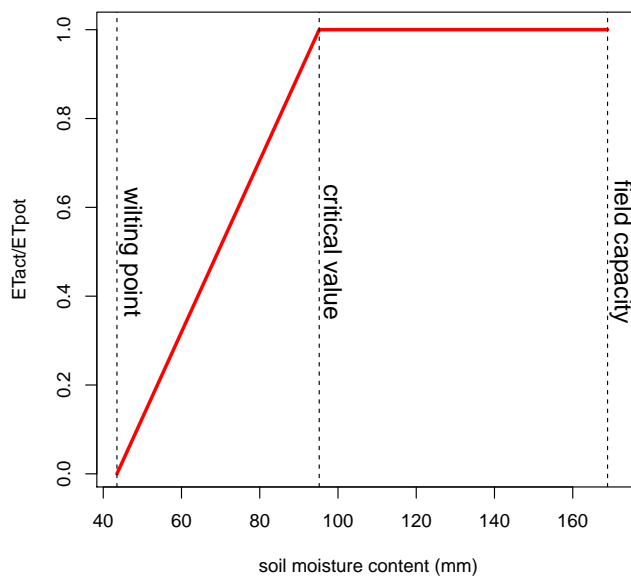
Soil reservoir SS

Inflow into the soil reservoir can either be from the snow pack reservoir (Q_{sm}) or directly from precipitation in the form of rain (P_{ra}). Outflow from this reservoir can either be recharge (Rch) or actual evapotranspiration ET_A . These last two terms both depend on the soil type and the associated soil storage SS . In this study one soil type over the whole globe is assumed: a light silty loam soil (Wösten *et al.*, 2001). The soil moisture stored at different dryness stages for this particular soil are given in Table 7. The soil is assumed to have a topsoil of 30 cm, a subsoil of 70 cm and a rooting depth of 50 cm.

ET_A depends on ET_P and the moisture storage in the soil reservoir. If this is above the critical soil moisture value, ET_A is equal to ET_P . Below this critical value, the ET_A decreases with a linear function (Figure 4). The other loss term in the soil reservoir is groundwater recharge Rch . If the soil reservoir is at field capacity, water flows directly to the groundwater reservoir. Some recharge already takes place when the soil storage is between critical value and field capacity due to gravitational force.

Table 7: Soil moisture stored at different dryness stages

Field Capacity	168.9 mm
Critical Point	95.2 mm
Wilting Point	43.5 mm

Figure 4: Relation between soil moisture stages and ET_A .

Groundwater reservoir

In this model, the groundwater reservoir is approached as a linear reservoir in which storage determines the outflow. The incoming term is recharge (Rch) and the outgoing term groundwater discharge (Q_{out}), calculated for $\Delta t = 1$:

$$Q_{out}(t) = Q_{out}(t - \Delta t) * e^{-\frac{1}{j}} + Rch(t) * \Delta t * (1 - e^{-\frac{1}{j}}) \quad (21)$$

Equation 21 is the de Zeeuw-Helling equation (Ritzema, 1994) which gives the relation between Q_{out} and Rch . The outflow from this linear reservoir is controlled through the ' j ' parameter, a reservoir coefficient (Kraijenhoff van de Leur, 1958). If j is higher, the water will be discharged slower:

$$j = \frac{1}{\pi^2} * \frac{\mu L^2}{kD} \quad (22)$$

j = reservoir coefficient	(/day)
μ = porosity	(-)
L = width reservoir	(m)
k = transmissivity	(m/day)
D = depth	(m)

j is kept constant at $250 d^{-1}$ for all the points in this study, which reflects an intermediate response of groundwater discharge to recharge. In fact, this reservoir generates a delay and attenuation between groundwater recharge and groundwater discharge.

Bypass

Next to the pathway through all the reservoirs there is also a bypass in the NUT_DAY model. This bypass is for rainfall that immediately flows to the groundwater reservoir, for example through cracks in a heavy clay soil if the soil moisture content is below the critical point. In this light silty loam soil this bypass took place.

2.4 Defining Droughts

After obtaining the time series of reference evapotranspiration, actual evapotranspiration, groundwater recharge and groundwater discharge per cell for the two different ET_0 methods, drought events in the period 1958-2001 were identified. To identify drought in this study, the variable threshold (VT) method (Hisdal *et al.*, 2004) is applied to the groundwater discharge (Wanders *et al.*, 2010). If the groundwater discharge is below the threshold, that time step is defined as drought. A monthly VT has been used, this means that for every month a threshold is defined, in total twelve thresholds. The threshold in this study equals Q_{80} , implying that a period is designated as drought as soon as the groundwater discharge is in the lowest 20% of all simulated discharges for that particular month. As a consequence, every location has dry conditions 20% of the time when the threshold is determined over the complete time period. To obtain this Q_{80} threshold, for every cell individually all data from one month over the period 1958-2001 are ranked. Subsequently, the 20th percentile is calculated and defined as threshold for that month in that cell. To smooth the threshold and overcome problems at the boundaries between two months, a daily moving average of the variable threshold is taken (Van Loon *et al.*, 2010; Wanders *et al.*, 2010). Thus, the threshold varies per day and per cell, but is kept constant over the years. Figure 5 gives an example of the smoothed monthly variable threshold and the periods indicated as drought anomalies. After identifying the drought periods per cell, drought characteristics can be determined; number, duration, intensity and standardized deficit volume. Note that droughts at the start of 1958 and at the end of 2001 are of unknown length. Especially in the climates with very long drought periods this can lead to distortion of the results.

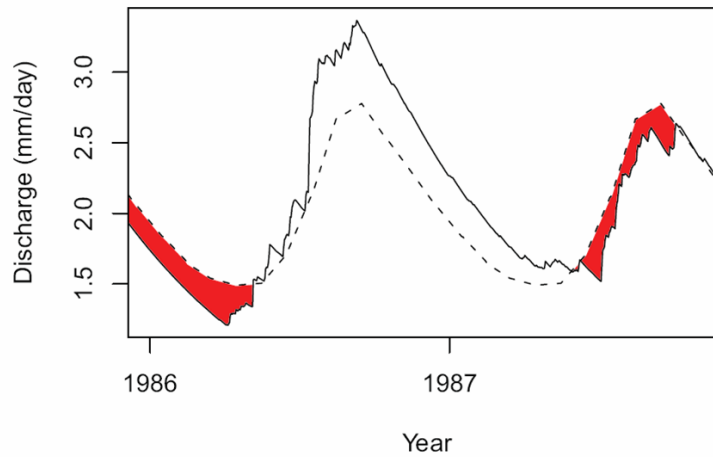


Figure 5: A daily smoothed monthly variable threshold, red colored periods indicate drought (Van Loon *et al.*, 2010; Wanders *et al.*, 2010).

Deficit volume

The deficit volume is the water shortage in a drought event (Hisdal *et al.*, 2004; Tallaksen *et al.*, 2009). Shortage is defined as the lack of available water (in this study the groundwater discharge) below the defined threshold level and determined by subtracting the Q_{out} from the threshold τ_t .

$$D(t) = \begin{cases} (\tau_t - X(t)) * \Delta t & \text{for } X(t) < \tau_t \\ 0 & \text{for } X(t) \geq \tau_t \end{cases} \quad (23)$$

2.4 Defining Droughts

$D(t)$ = deficit volume at time step t	(mm)
τ_t = threshold level at time step t	(mm/day)
$X(t)$ = groundwater discharge Q_{out} at time step t	(mm/day)
Δt = length time step	(day)

$$V_j = \sum_{t_s}^{t_e} D(t) \quad (24)$$

V_j = deficit volume for drought j	(mm)
$D(t)$ = deficit volume per time step t	(mm)
t_s = start of drought	(-)
t_e = end of drought	(-)

Duration

Duration is the time that a certain drought lasts, so the sum of time steps that there is an uninterrupted drought. In this period the groundwater discharge is constantly below the threshold level.

$$L_j = \sum_{t_s}^{t_e} \max\{1_{X(t) < \tau_t}\} \quad (25)$$

L_j = length of drought j	(day)
$1_{X(t) < \tau_t}$ = indicator function; 1 if there is drought, 0 if there is no drought	(-)

Intensity

The intensity of a drought is the deficit per unit time, and is therefore easy to obtain with the above equations:

$$I_j = \frac{V_j}{L_j} \quad (26)$$

Standardized Deficit Volume

To determine the deficit volume relative to the groundwater discharge, the standardized deficit volume is calculated. This is done to compare different locations which have a very different groundwater discharge. The standardized deficit volume gives the deficit volume (mm) standardized by the average groundwater discharge (mm/day):

$$St.Def.Volume = \frac{V_j}{\overline{Q_{out}}} \quad (27)$$

$St.Def.Volume$ = Standardized Deficit Volume	(day)
$\overline{Q_{out}}$ = Average groundwater discharge	(mm)

After finishing the processing, in every cell for every day in the period 1958-2001 all water balance components plus all drought characteristics are known. For the analysis in the next chapter, the daily data for evapotranspiration are aggregated to monthly data. The drought analysis is still based on daily ET_0 , ET_A and Q_{out} data.

3 Results

ET_0 has been calculated with the radiation-based and temperature-based method of Penman-Monteith with grass as reference crop. Because for the reference crop the crop factor $K_c = 1$ (Allen *et al.*, 1998), ET_P is equal to ET_0 (except for situations with snow cover or no sunrise, see Section 2.3). Therefore, only ET_0 and ET_A are discussed in this chapter. From ET_0 , ET_A was calculated using soil moisture storage simulated with the NUT_DAY model. Finally, with this model the groundwater discharge was obtained. By formulating a variable threshold per month per location, periods of drought based on groundwater discharge were identified. In this section the results from this full analysis are presented, first for all climates taken together and thereafter per major climate and for northern and southern hemisphere separately. On the northern hemisphere, summer is from April until September, on the southern hemisphere from October until March. Winter on the northern hemisphere is from October till March, and from April till September on the southern hemisphere.

3.1 Overview all climates

Goal of this research was, among others, to investigate the difference between two different methods to estimate reference evapotranspiration; a radiation-based and a temperature-based type (ET_{0rad} and ET_{0temp} respectively). In the following analysis all 1495 sampled cells are taken into account, hence all climatic regions. First the results for evapotranspiration will be discussed, followed by the results concerning hydrological drought.

3.1.1 Evapotranspiration

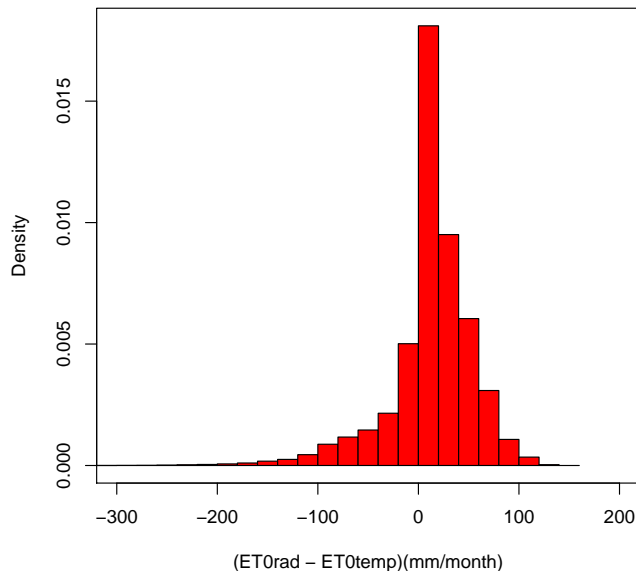


Figure 6: Difference in reference evapotranspiration between the two methods for all 1495 cells.

Figure 6 gives an overview of the difference in ET_0 between the two methods. This histogram is based on all months in the period 1958-2001 in all 1495 cells, so all climates. Please note that this graph shows the density, so the relative frequency divided by the class width. This implies that the sum of all densities times class width is one. The mean difference is 11.6 mm/month, the mean absolute difference is 31.1 mm/month. 46% of the selected cells have differences between -20 and +20 mm/month. The difference can be up to more than 300 mm/month; it varies between -336 mm/month and 142 mm/month. In this figure it seems that the radiation-based method is higher, i.e. 76% of the differences are in the right region of zero. To place this difference more in a context (i.e.

consideration of large differences in ET_0 across the globe), the standardized difference (st.difference) is also computed. The st.difference is obtained by dividing the difference between ET_{0rad} and ET_{0temp} by ET_{0rad} . Figure 7 shows the st.difference. For example, a standardized difference of +0.25 says that the monthly difference between the two methods equals 25% of the monthly ET_{0rad} , and that ET_{0rad} is larger than ET_{0temp} . 30% of the cells is within the range of -0.25 and +0.25 (Appendix

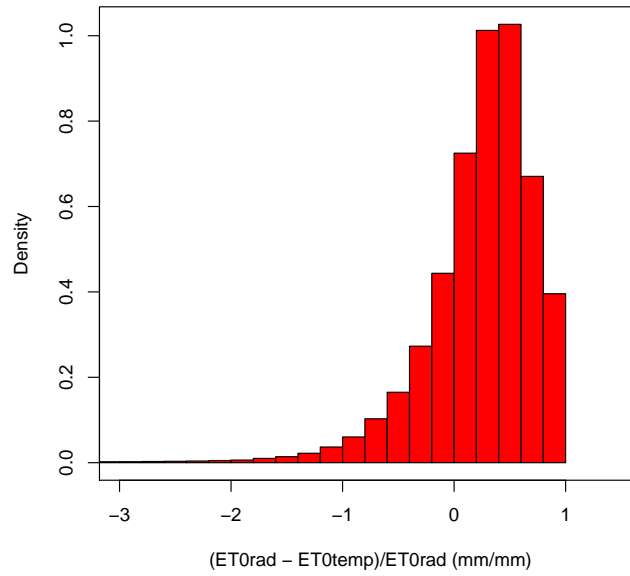


Figure 7: Standardized difference in ET_0 between the two methods for all 1495 cells.

F.1). Notable is that the st.difference on the right hand side of zero is bounded by 1. This implies that the ET_{0temp} in this case was zero.

For hydrological drought and associated water resources, not reference evapotranspiration ET_0 but actual evapotranspiration ET_A is more relevant. Also for ET_A a difference graph is drawn, Figure 9.

By comparing Figures 9 and 6 one can see that the differences between the two methods are

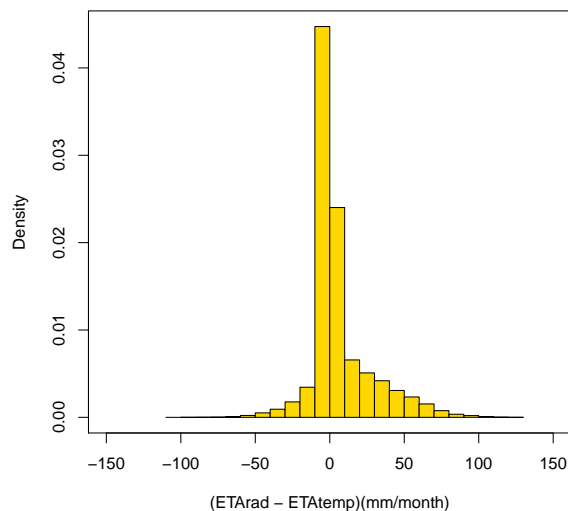


Figure 9: Difference between the two methods in ET_A for all 1495 cells.

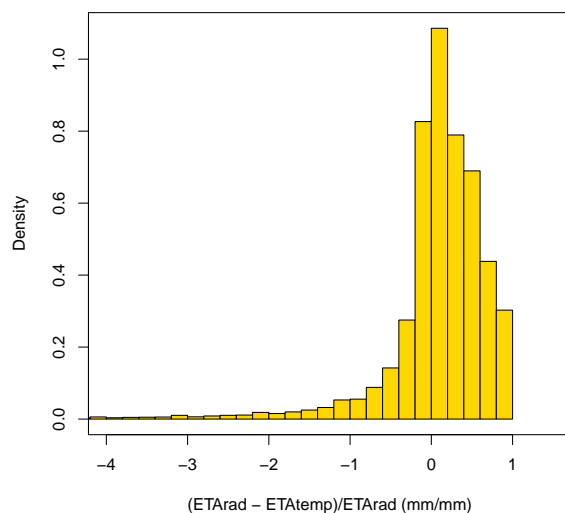


Figure 10: Standardized difference between the two methods in ET_A for all 1495 cells.

substantially lower for ET_A . The mean difference is 7.1 mm/month, the mean absolute difference 11.4 mm/month. An interesting feature is that the highest frequency is now in the region below zero ($ET_{Atemp} > ET_{Arad}$), while for ET_0 this was in the region above zero. Now only 48% of the differences are in the region above zero. 79% of all differences are within the range -20 mm/month and +20 mm/month. In the st.difference graph of ET_A (Figure 10), 41% of the standardized differences lie within the range -0.25 and +0.25. Also for ET_A the highest 1% above and below zero are selected, to investigate which climates are present in the highest difference class. In Figure 11 a clear difference with ET_0 is visible. Almost all climates are present on both sides of the extremes for ET_A .

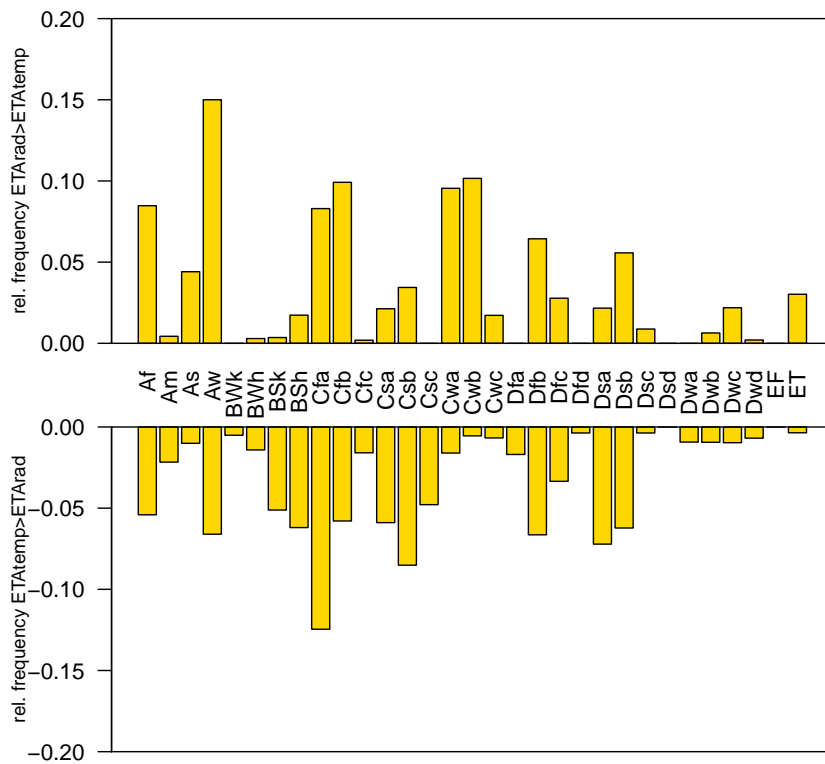


Figure 11: Relative frequency of climates in highest 1% of difference class. In the upper graph radiation-based ET_A is higher than temperature-based ET_A , in the lower graph temperature-based ET_A is higher.

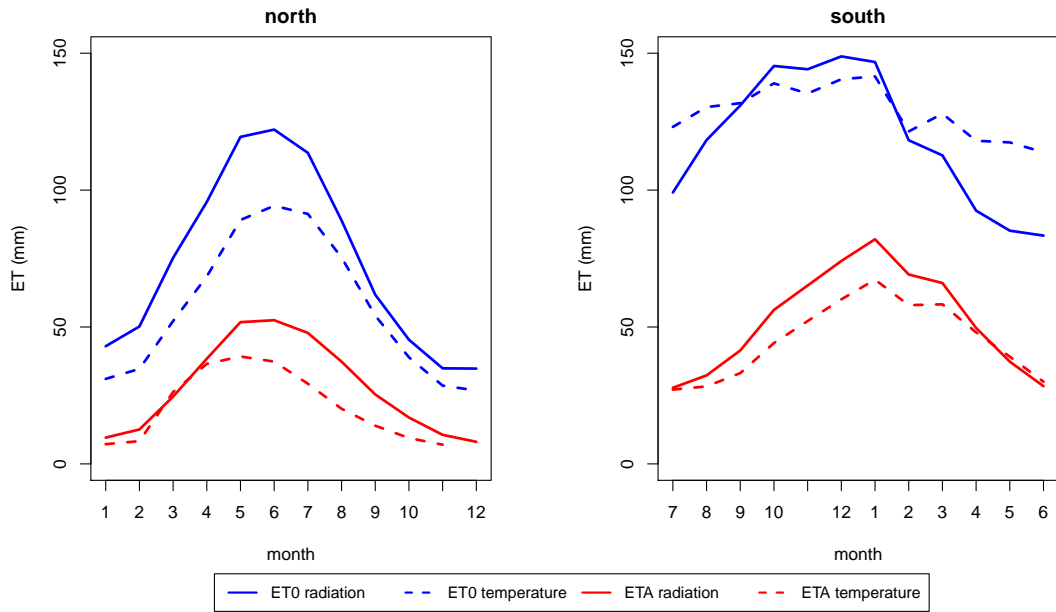


Figure 12: Mean monthly evapotranspiration for all cells over the whole period 1958-2001, note difference in x-axis.

Figure 12 shows the mean monthly regime for both ET_0 and ET_A for all 1495 cells over the complete period 1958-2001. A division is made between the northern and southern hemisphere, because of the seasonality which would lead to interference of the data. Both the ET_0 and ET_A of the southern hemisphere are higher than of the northern hemisphere. This is associated with the locations of the cells on the globe (see below). The figure shows that on the northern hemisphere for ET_0 the radiation-based method is on average higher, while this is for about half of the year the other way around on the southern hemisphere. For ET_A both methods alternate, although it seems that in general the radiation-based method leads to higher estimations for ET_A . It also shows that the differences between the ET_A according to the two methods are in absolute sense smaller than for ET_0 , but relatively larger. Seasonality is less clear visible in the southern hemisphere. An explanation could be that the WFD cells in the southern hemisphere are less well divided over the whole latitude than the northern hemisphere, see Figure 13. It can very well be the case that the climates with strong seasonality are not or only in a small number present within the WFD for the southern hemisphere. 80.5% of all cells are in the northern hemisphere (Section 2.1). The next section will explore the consequences for hydrological drought and drought characteristics, based on the two different methods.

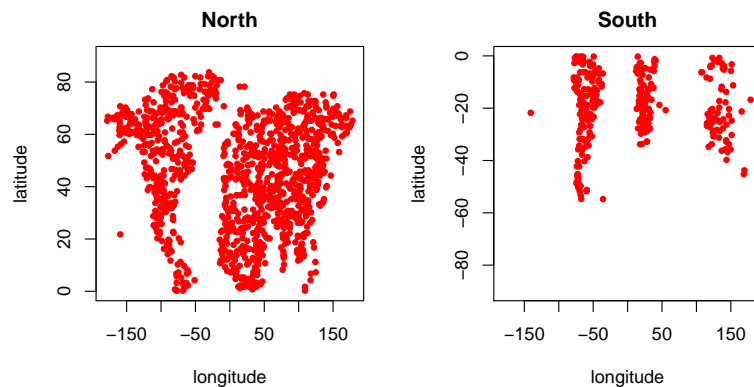


Figure 13: Spreading of the selected cells in the WFD for northern and southern hemisphere.

3.1.2 Hydrological Drought

As described in the previous chapter, hydrological drought is determined with a variable threshold (Section 2.4). After defining the droughts, several drought characteristics can be determined. Table 8 gives an overview of the drought characteristics for all 1495 cells. All the means have been calculated using all cells from all different climates (Table 8). The differences in drought characteristics between the two methods is also expressed as a percentage relative to the radiation-based method (last column). For all 1495 cells the average number of droughts is almost 8% lower for the temperature-based than for the radiation-based method. As a consequence of the drought definition (Section 2.4) and the associated negative correlation between number of drought and drought duration, the mean duration of a drought should be higher for the temperature-based method, i.e. 3%. Larger discrepancies exist in the other characteristics, as the table shows. With the temperature-based method, the mean deficit

Table 8: Absolute drought characteristics and difference relative to radiation-based method

Drought characteristic	Unit	Radiation	Temperature	Percentage
Number of Droughts	(-)	50.1	46.2	8%
Mean Duration	(days)	175.5	181.1	-3%
Mean Deficit Volume	(mm)	6.0	7.7	-29%
Mean Intensity	(mm/day)	0.03	0.04	-24%
Mean St.Deficit Volume	(day)	8.6	10.2	-18%

volume is significantly higher; almost 29%. However, the absolute values are more realistic, i.e. the mean deficit volume between the two methods differs not more than 1.7 mm. The Mean St.Deficit Volume for ET_{0rad} is 8.6 day. This implies that the mean deficit volume is 8.6 times the average discharge. The St.Deficit Volume for ET_{0temp} is 1.6 (10.2-8.6) times the average discharge higher. A study performed by Van Huijgevoort *et al.* (2011) compares in five different catchments the drought characteristics obtained with WFD and obtained with local forcing data. Also different models were used to simulate groundwater discharge. The differences in drought characteristics between the two forcing sets are in the same order of magnitude as the differences in Table 8 (see Appendix F.2). Differences in drought characteristics between simulated stream flow and observed stream flow are even higher (Van Huijgevoort *et al.*, 2011; Van Loon *et al.*, 2011). One should realize that the numbers in Table 8 are based on worldwide averaged forcing data which reduces small scale effects due to large sample size, while the numbers given in Van Huijgevoort *et al.* (2011) are derived from catchment scale studies.

3.2 Equatorial A Climates

The A-climates are the equatorial climates, with $T_{Mmin} \geq +18^{\circ}C$. There are four sub climates in this region (see Table 5). Explanation for the different parameters can be found in Table 4.

Table 9: sub climates in climate A, adapted from Kottek *et al.* (2006)

	Description	Criterion
Af	Rainforest Fully Humid	$P_{min} \geq 60mm$
Am	Monsoon	$P_{ann} \geq 25(100 - P_{min})$
As	Savannah Dry Summer	$P_{min} < 60mm$ in summer
Aw	Savannah Dry Winter	$P_{min} < 60mm$ in winter

3.2.1 Evapotranspiration

Figure 14 shows the differences in ET_0 for the two methods for the 235 cells belonging to this major climate type (Table 5). The absolute mean difference of climate A is 37.6 mm/month, the mean difference 30.6 mm/month. More than 76% of the differences are larger than zero, implying that in general the radiation-based method leads to higher ET_0 estimations in the A climates. Differences in reference evapotranspiration vary between +129.0 mm/month ($ET_{0rad} > ET_{0temp}$) and -133.9 mm/month ($ET_{0temp} > ET_{0rad}$). Only 25% of the differences falls within the range -20 and +20 mm/month. The standardized difference of ET_0 (Appendix A.1) varies between -2.04 and +0.95, and

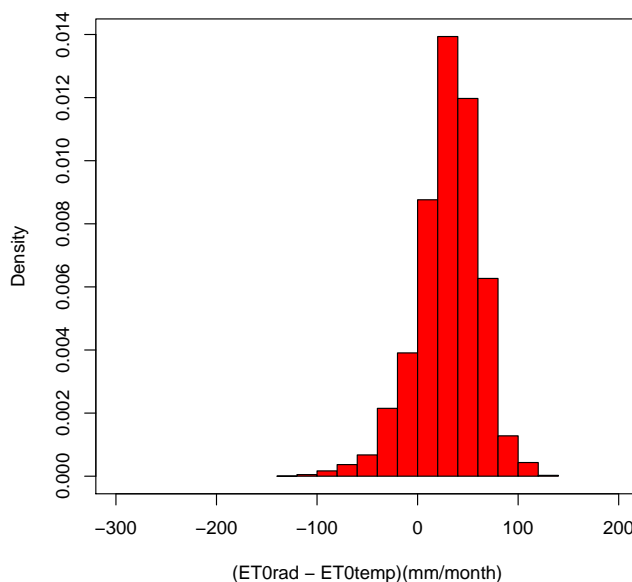


Figure 14: Differences in ET_0 between radiation-based and temperature-based method for climate A.

42% of the differences lie within the range -0.25 and +0.25. Appendix A.1 also shows that the largest variation in differences between the two methods exists in sub climate Aw, this climate is present in the highest 1% differences higher than zero, and present in the highest 1% differences lower than zero. For the actual evapotranspiration ET_A , see Appendix A.2, the absolute average difference between the two methods is lower than for ET_0 ; 22.0 mm/month. However, it is striking that the maximum difference is still +129 mm/month for the region above zero. For the region below zero this is -105.3 mm/month. For ET_A 69% of the differences is above zero. 57% of the differences for ET_A lie within the range -20 mm/month and +20 mm/month. For the standardized difference of ET_A (Appendix

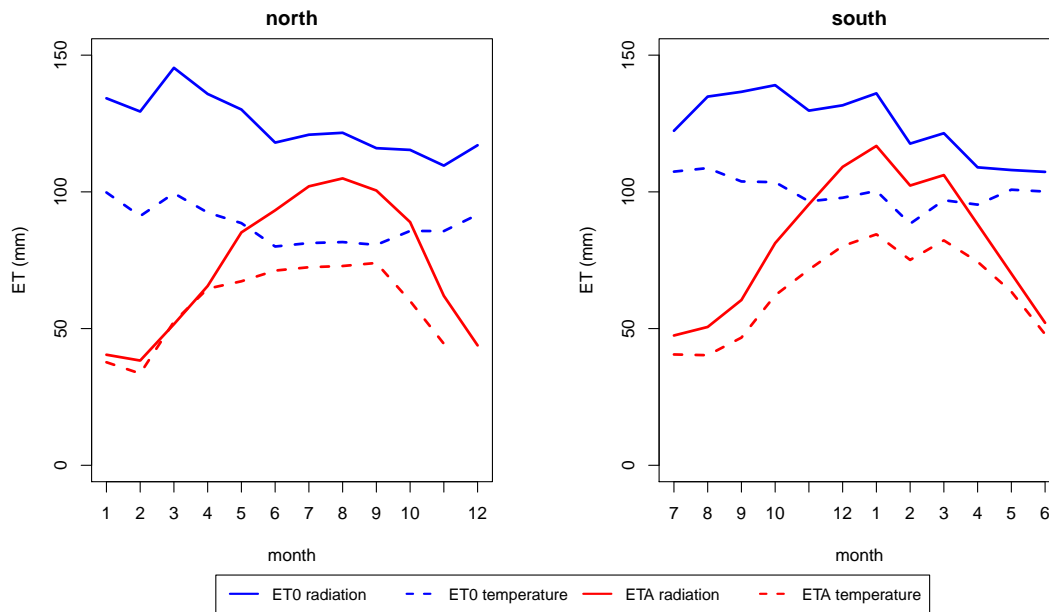


Figure 15: Mean monthly evapotranspiration of the cells with major climate A, divided over northern and southern hemisphere. Note difference in x-axis.

A.2), 52% lies within the range -0.25 to $+0.25$. Within the sub climates of major climate A, the largest differences occur in the Aw and the Af climate (see Appendix A.1 and A.2)

Figure 15 shows the mean monthly ET_0 and ET_A for all cells with major climate A. 51.5% of all cells with climate A is in the northern hemisphere, 48.5% in the southern hemisphere. The radiation-based method leads for ET_0 as well as for ET_A both for the northern and the southern hemisphere to higher evapotranspiration numbers. ET_A shows a clear seasonality, which is absent in ET_0 .

3.2.2 Hydrological Drought

The discrepancy between the mean number of droughts in climate A for the two different methods is rather small: only 2% (Table 10). The mean intensity of the drought differs 16% within the A climate, the mean standardized deficit volume on the contrary only 1%. Notable is that, except from the number of droughts, the temperature-based method leads to higher numbers for the drought characteristics. Within the sub climates, the temperature-based method also leads to higher numbers for the drought characteristics. This pattern is only broken by the Af climate (see Appendix A.3), in which the standardized deficit volume is +10.3%, so higher for the radiation-based method.

Table 10: Drought characteristics and difference relative to radiation-based method, climate A

Drought characteristic	Unit	Radiation	Temperature	Difference
Number of Droughts	(-)	59.6	58.3	2%
Mean Duration	(days)	59.0	60.0	-2%
Mean Deficit Volume	(mm)	15.5	17.7	-14%
Mean Intensity	(mm/day)	0.07	0.08	-16%
Mean St.Deficit Volume	(day)	6.1	6.1	-1%

3.3 Arid B Climates

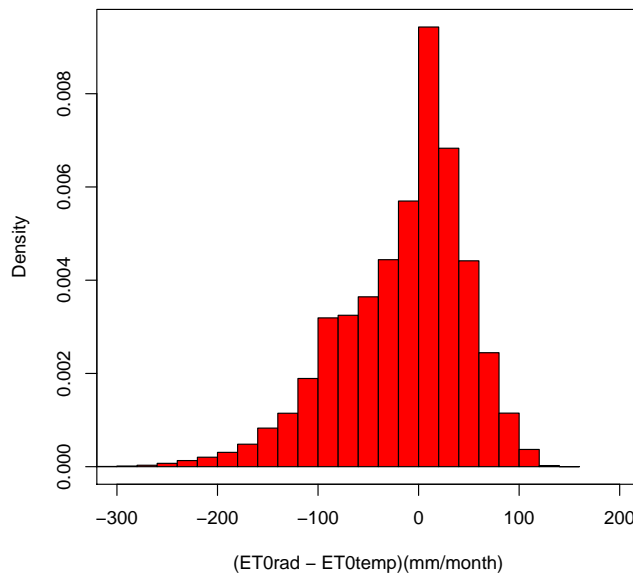
The B-climates are the arid climates, so with in general very dry conditions. The criterion for a B-climate is $P_{ann} < 10P_{th}$ (see Table 4). 313 cells are selected for this major climate type (Table 5) Within the B-climates, four different sub climates are distinguished (see also Table 5).

Table 11: sub climates in climate B, adapted from Kottek *et al.* (2006)

	Description	Criterion
W	Desert climate	$P_{ann} \leq 5P_{th}$
S	Steppe climate	$P_{ann} > 5P_{th}$
h	Hot	$T_{ann} \geq 18^{\circ}C$
k	Cold	$T_{ann} < 18^{\circ}C$

3.3.1 Evapotranspiration

Based on Figure 8 the expectation is that for the B-climates the center of gravity is more in the left hand side of the zero in the difference histogram. This is true, but probably not as much as expected: 49% of the differences lie in the right region ($ET_{0rad} > ET_{0temp}$), 51% in the left region ($ET_{0temp} > ET_{0rad}$). The mean absolute difference between the two methods is 48.5 mm/month, while the mean difference is -15.5 mm/month. 30% of all the differences lie in the range -20 and +20 mm/month. The differences vary between -336.2 and +142.4 mm/month. For the standardized

Figure 16: Differences in ET_0 between radiation-based and temperature-based method for climate B.

difference of ET_0 (Appendix B.1), 40% of the differences lie in the range -0.25 and +0.25. Appendix B.1 also shows that all the sub climates in major climate B are present in the highest 1% differences on both sides. For the actual evapotranspiration, ET_A , the agreement among the methods is much higher (Appendix B.2). 32% of the differences are zero! The remaining differences are small and again equally divided over the left and right region (no bias). The mean absolute difference for ET_A is 3.1 mm/month, while the mean difference is 0.2 mm/month. 96% of all the differences are within the range -20 and +20 mm/month. It seems that both methods on average cancel each other out. For the standardized ET_A (Appendix B.2) up to 72% of the standardized differences falls within the range -0.25 and +0.25.

Figure 17 shows the mean monthly ET_0 and ET_A for all cells with major climate B. 73.2% of all the cells with climate B are in the northern hemisphere. Notable is that for these B climates, the temperature-based method leads on average to higher ET_0 than the radiation-based method. On the southern hemisphere this is stronger than on the northern hemisphere. For ET_A both methods in both hemispheres seem to agree quite well. Appendix B.2 shows the mean monthly evapotranspiration per sub climate of major climate B. Notable is that especially in the southern region the temperature-

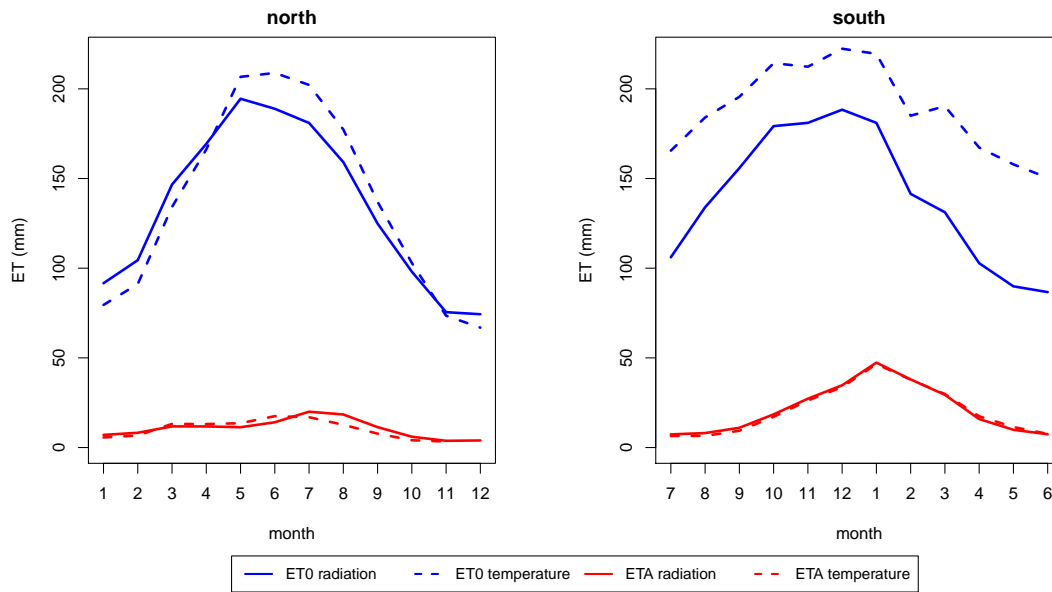


Figure 17: Mean monthly evapotranspiration of the cells with major climate B, divided over northern and southern hemisphere. Note difference in x-axis.

based method shows much less seasonality than the radiation-based method. Especially in the southern hemisphere the temperature-based method leads to higher estimations of ET_0 than the radiation-based method (e.g. BWk). For each sub climate differences in ET_A are minor.

3.3.2 Hydrological Drought

The differences between the two methods are relatively small for ET_A , which leads to the expectation that for drought the differences are minor as well. This is the case, the largest discrepancy between the two methods when looking at climate B in general is -10% in the mean deficit volume (Table 12). Overall can be concluded that the relative differences in drought characteristics are small, in particular when compared to Appendix F.2.

Looking at the sub climates (Appendix B.3), the largest differences between the two methods seem to exist in the Steppe climates, especially BSh. For the two desert climates (BWh, BWk), all differences are far below 3%.

Table 12: Drought characteristics and difference relative to radiation-based method, climate B

Drought characteristic	Unit	Radiation	Temperature	Difference
Number of Droughts	(-)	36.8	36.0	2%
Mean Duration	(days)	339.8	343.1	-1 %
Mean Deficit Volume	(mm)	2.1	2.4	-10%
Mean Intensity	(mm/day)	0.01	0.01	-4%
Mean St.Deficit Volume	(day)	12.0	12.1	-2%

Special notion should be taken of the fact that the number of droughts times the average duration of a drought event is much higher than 20% of the time, what it should be according to the variable threshold method (Section 2.4). This is caused by the large variation within climate B. Appendix F.2 shows that for the B-climates the spread in duration and number of droughts is very large. Per individual cell there is drought 20% of the time, but averaged over all cells this is no longer a linear relationship. Next to that the begin and end drought (explained in Section 2.4) are excluded, which has large influence in the cells with long droughts.

3.4 Warm temperate C Climates

The C-climates are the warm temperate climates with climate criterion $-3^{\circ}\text{C} < T_{min} < +18^{\circ}\text{C}$, for explanation of the criteria, see Table 4. 242 cells are selected for this major climate type (Table 5). The C-climate distinguishes nine different sub climates, presented in Table 13.

Table 13: sub climates in climate C, adapted from Kottek *et al.* (2006)

	Description	Criterion
s	Dry summer	$P_{smin} < P_{wmin}, P_{wmax} > 3P_{smin}, P_{smin} < 40\text{mm}$
w	Dry winter	$P_{wmin} < P_{smin}, P_{smax} > 10P_{wmin}$
f	Fully humid	Neither Cs nor Cw
a	Hot summer	$T_{Mmax} \geq 22^{\circ}\text{C}$
b	Warm summer	Not a and at least 4 months $T_{mon} \geq 10^{\circ}\text{C}$
c	Cool summer, cold winter	Not a or b and $T_{Mmin} > -38^{\circ}\text{C}$

3.4.1 Evapotranspiration

For climate C, in general ET_{0rad} leads to higher numbers than ET_{0temp} (Figure 18). 72% of all the differences lie above zero, 28% below zero. The mean absolute difference is 38.7 mm/month, while the mean difference is 18.6 mm/month. Only 31% of all the differences between the two methods are within the range -20 and +20 mm/month. The differences vary between -182.2 and +138.9 mm/month. The graph of the standardized difference for ET_0 (Appendix C.1) shows that 26% of the

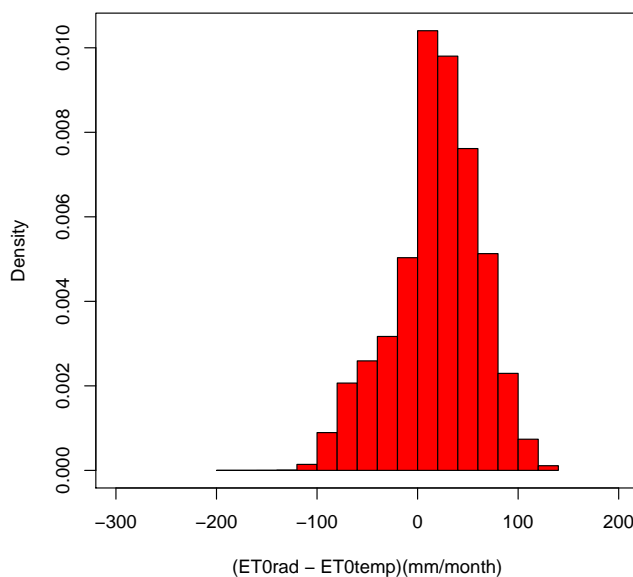


Figure 18: Differences in ET_0 between radiation-based and temperature-based method for climate C.

differences lie between -0.25 and +0.25. The different sub climates within major climate C are almost all present in the highest 1% of differences on both sides (Appendix C.1). Cfc and Cwc, so the climates with cool summer and cold winter, are absent. For ET_A (Appendix C.2), the mean difference is 11.7 mm/month, the mean absolute difference 20.4 mm/month. The differences vary between -96.9 and +123.0 mm/month, so especially for $ET_{Atemp} > ET_{Arad}$ the differences have become much smaller. 65% of the differences is above zero ($ET_{Arad} > ET_{Atemp}$), 34% below zero, 1.5% of the differences equals zero. 62% of all differences can be found in the range -20 and +20 mm/month. For the standardized difference of ET_A (Appendix C.2) 38% of the differences is within the range -0.25 and +0.25 mm/mm. So, again a decrease in standardized differences takes place from ET_0 to ET_A .

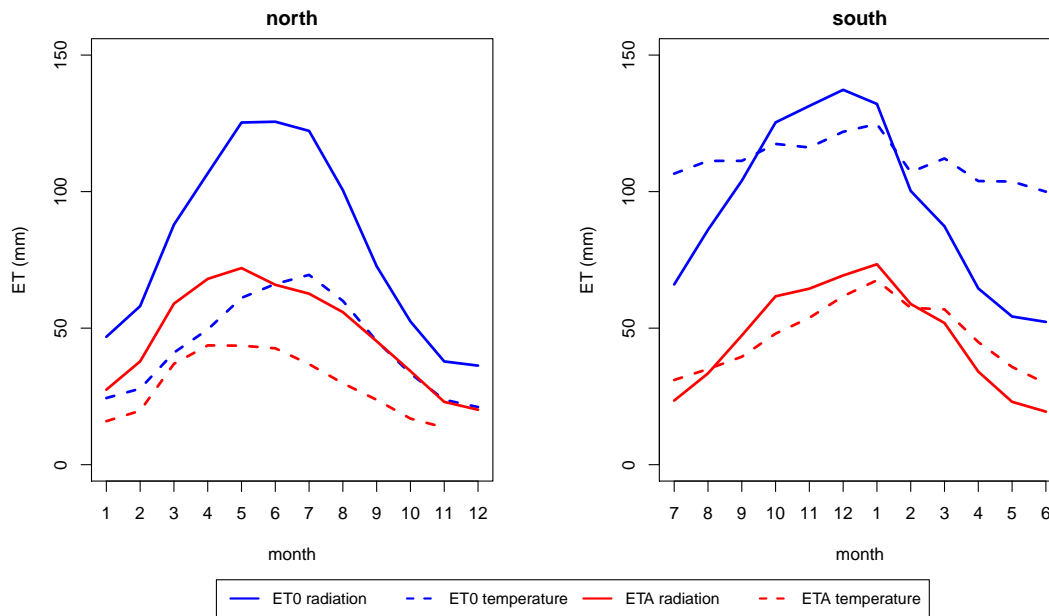


Figure 19: Mean monthly evapotranspiration of the cells with major climate C, divided over northern and southern hemisphere. Note difference in x-axis.

Figure 19 shows the mean monthly ET_0 and ET_A for all cells with major climate C. Of the cells with major climate C 64.9% is situated in the northern hemisphere. Notable in this graph is that in the northern hemisphere the ET_{0rad} leads to much higher values than ET_{0temp} , but in the southern hemisphere this alternates for part of the year with the temperature-based method. The same holds for ET_A . Especially in the southern hemisphere the temperature-based method for ET_0 has less seasonality than the radiation-based method.

3.4.2 Hydrological Drought

The average number of droughts in the period 1958-2001 for climate C is 63.4 for the radiation-based method, and 61.6 for the temperature-based method (Table 14). The C-climate is from the five major climates the climate with the highest number of droughts, with the corollary that the mean duration is shortest of all climates.

Table 14: Drought characteristics and difference relative to radiation-based method, climate C

Drought characteristic	Unit	Radiation	Temperature	Difference
Number of Droughts	(-)	63.4	61.6	3%
Mean Duration	(days)	55.5	60.1	-9 %
Mean Deficit Volume	(mm)	8.0	9.9	-24%
Mean Intensity	(mm/day)	0.05	0.06	-22%
Mean St.Deficit Volume	(day)	5.7	6.2	-9%

Differences between the two methods in the drought characteristics especially exist in the mean deficit volume and mean intensity, as Table 14 shows.

The different sub climates within climate C differ largely from each other (Appendix C.3). For the numbers of droughts for example, Csa has a difference of +25%, while Csc has a difference of -27%. The smallest differences occur in the fully humid climates Cf, the highest in the dry summer sub climates Cs. Within these climate subtypes the climates with temperature criterion 'cool summer and cold winter' have the highest differences.

3.5 Snow D Climates

The D climates are the snow climates with temperature criterion $T_{min} \leq 3^{\circ}C$ (see Table 4 and 5). 506 cells are selected for this major climate type (Table 5). Within this major climate, twelve sub climates exist.

Table 15: sub climates in climate D, adapted from Kottek *et al.* (2006)

	Description	Criterion
s	Dry summer	$P_{smin} < P_{wmin}, P_{wmax} > 3P_{smin}, P_{smin} < 40mm$
w	Dry winter	$P_{wmin} < P_{smin}, P_{smax} > 10P_{wmin}$
f	Fully humid	Neither Ds nor Dw
a	Hot summer	$T_{Mmax} \geq 22^{\circ}C$
b	Warm summer	Not a and at least 4 months $T_{mon} \geq 10^{\circ}C$
c	Cool summer and cold winter	Not a or b and $T_{Mmin} > -38^{\circ}C$
d	Extremely continental	Not a or b and $T_{Mmin} \leq -38^{\circ}C$

3.5.1 Evapotranspiration

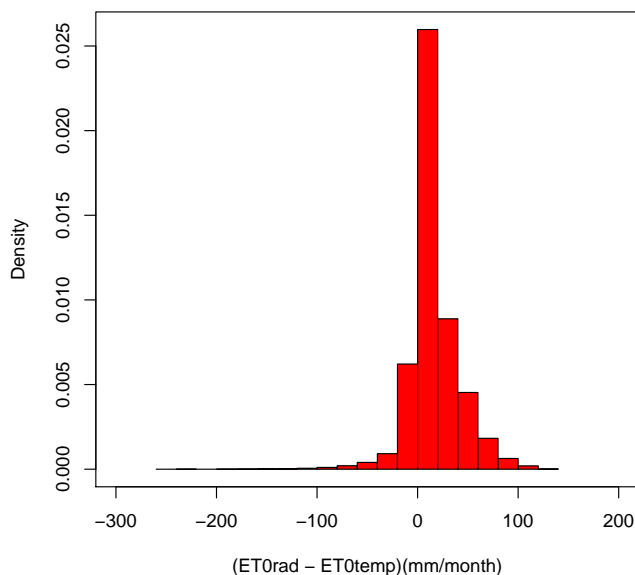


Figure 20: Differences in ET_0 between radiation-based and temperature-based method for climate D.

For climate D the radiation-based method gave in 84% of the cases a higher evapotranspiration than the temperature-based method. They only agreed on 0.6% of the cases. The absolute mean difference is 19.6 mm/month, the mean difference 15.1 mm/month. The frequency of differences is shown in Figure 20. 64% of all the differences lie within the range -20 and +20 mm/month. The differences vary between -244.8 and 131.4 mm/month. For the standardized difference, 28% of the standardized differences lie within the range -0.25 to +0.25 for ET_0 (see Appendix D.1). Appendix D.1 also shows that the sub climates in major climate D are not all present in the highest 1% of differences, some are in the region $ET_{0rad} > ET_{0temp}$, like Dsb and Dsc, and others are in the region $ET_{0temp} > ET_{0rad}$, like Dfa and Dfb.

For ET_A (Appendix D.2) the mean difference is 5.3 mm/month, the mean absolute difference 9.3 mm/month. The variation in differences is between -83.5 and +127.5 mm/month. Especially for cells with $ET_{Atemp} > ET_{Arad}$, numbers have going down from ET_0 to ET_A . For ET_A , 32% of

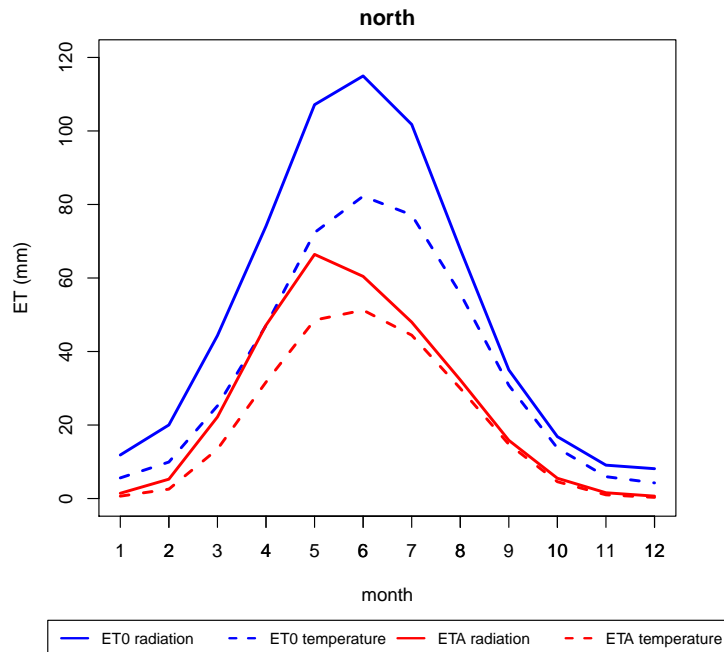


Figure 21: Mean monthly evapotranspiration of the cells with major climate D.

the differences equals zero. 83% of all differences lie in the range -20 and +20 mm/month. The standardized differences of ET_A (Appendix D.2) are for 60% in the range -0.25 and +0.25.

Figure 21 shows the development of ET_0 and ET_A over a year. For the D-climates, no division between north and south is made because none of the selected cells with climate D lies in the southern hemisphere. The largest discrepancy between the two methods exists in the summer period (May-July), later on the two methods agree upon each other much more. On average the radiation-based method leads to higher estimations of ET_0 as well as ET_A . Note that ET_P is set to zero as soon as there is snow cover (for ET_0 this not necessarily has to be the case). Therefore, ET_A also equals zero when the soil is covered with snow.

3.5.2 Hydrological Drought

There is a notable discrepancy in the number of droughts between the two different methods: the radiation-based method leads to on average 56.2 droughts, whereas for the temperature-based methods only 47.7 droughts are found (Table 16). This difference can also be observed in all the other drought characteristics. The differences in drought characteristics in climate D are relatively large compared to other climates.

Also in the sub climates large differences are found, see Appendix D.3. The number of droughts is in all cases higher for the radiation-based method than for the temperature-based method. For the Ds-climates (dry summer) the difference is on average the highest. There is no clear pattern within the sub climates for which the highest discrepancies exist, but the sub climate with the largest difference is Dwd, dry winter and extremely continental. For the mean deficit volume this difference is even up to -225%!

3.6 Polar E Climates

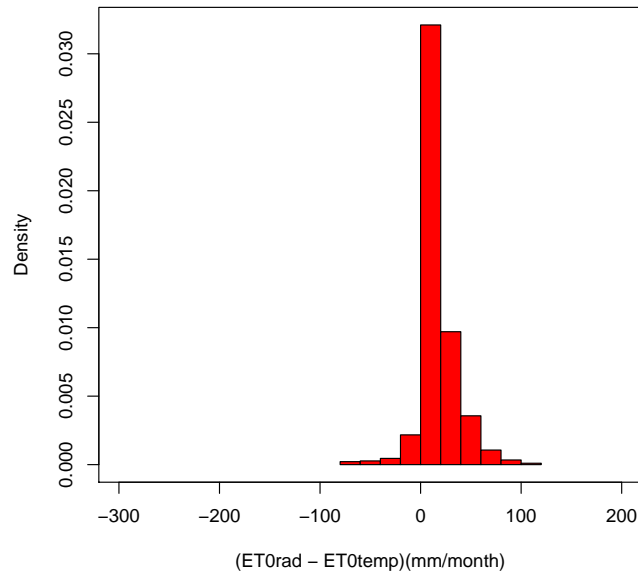
The E climates belong to the polar areas of the world, with $T_{max} < +10^\circ C$ (see Table 4). 199 cells are selected for this major climate type (Table 5) This climate contains two sub climates (see also Table 5).

Table 16: Drought characteristics and difference relative to radiation-based method, climate D

Drought characteristic	Unit	Radiation	Temperature	Difference
Number of Droughts	(-)	56.2	47.7	15%
Mean Duration	(days)	61.7	75.9	-23 %
Mean Deficit Volume	(mm)	3.7	5.8	-56%
Mean Intensity	(mm/day)	0.02	0.03	-37%
Mean St.Deficit Volume	(day)	6.3	8.5	-34%

Table 17: sub climates in climate E, adapted from Kottke *et al.* (2006)

	Description	Criterion
EF	Frost climate	$T_{Mmax} < 0^{\circ}C$
ET	Tundra climate	$0^{\circ}C \leq T_{Mmax} < +10^{\circ}C$

Figure 22: Differences in ET_0 between radiation-based and temperature-based method for climate E.

3.6.1 Evapotranspiration

For the polar climates, it is quite clear which method leads to a higher estimation of ET_0 , i.e. 94% of the differences are above zero, so $ET_{0rad} > ET_{0temp}$ (Figure 22). The absolute mean difference is 16.2 mm/month, the mean difference 14.3 mm/month. 69% of all the differences lie in the range -20 and +20 mm/month. The differences vary between -76.4 and 119.6 mm/month. Although the numbers for the differences may look small in comparison with other climates, the standardized difference is not that low, because of the low ET_0 in this cold climate. Only 8% of all the standardized differences lie within the region -0.25 and +0.25 for ET_0 (Appendix E.1). Appendix E.1 also shows that the biggest differences occur in the ET-climate, and not in the EF climate.

For ET_A (Appendix E.2) the differences are much smaller, on average the difference is 5.5 mm/month and the absolute average is 6.3 mm/month. They vary between -58.8 +100.1 mm/mm. 87% of all the differences are in the region -20 and +20 mm/month. The standardized differences of ET_A (Appendix E.2) within the range -0.25 and +0.25 extremely increased from 8% (ET_0) to 68%, the largest increase of all climates.

Figure 23 shows the development of ET_0 and ET_A averaged over a year. 96.0% of all cells with

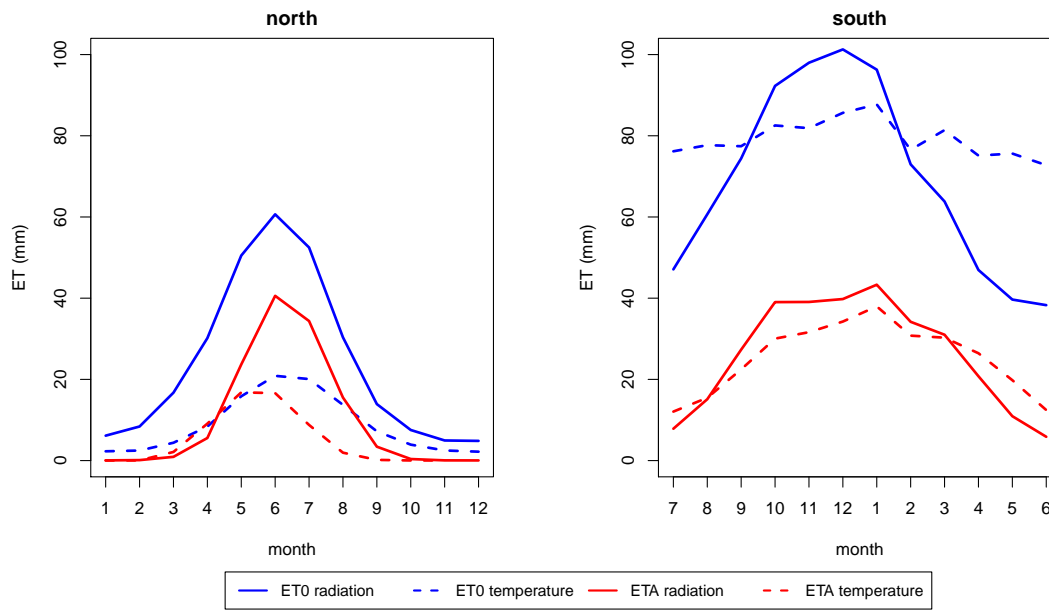


Figure 23: Mean monthly evapotranspiration of the cells with major climate E, divided over northern and southern hemisphere. Note difference in x-axis.

climate E lie in the northern hemisphere, so the graph of the southern hemisphere is only based on 4% (8 cells) of all climate E cells. The largest discrepancies exist during the summer month. Again it seems that the temperature-based method shows less seasonality, so is more constant throughout the year, than the radiation-based method. On the southern hemisphere this leads to higher values with the temperature-based method in the winter period. For ET_A both methods alternate on both hemispheres.

One should realize that the E-climate is the climate that contains cells where there is no sunrise during some time of the year (polar climates). For these periods, the temperature-based method has an ET set to zero (see Section 2.2.2). In the Southern hemisphere none of the selected cells is on these high latitudes, while on the northern hemisphere there are plenty of cells with a latitude higher than 60° , implying that they potentially meet the criterion of no sunrise and therefore no evapotranspiration. This can explain the large difference in evapotranspiration between the northern and the southern hemisphere. Next to that, ET_P and subsequently ET_A is set to zero as soon as the soil is covered with snow. This does not hold for ET_0 and can therefore partly explain the difference between ET_0 and ET_A .

3.6.2 Hydrological Drought

Table 18: Drought characteristics and difference relative to radiation-based method, climate E

Drought characteristic	Unit	Radiation	Temperature	Difference
Number of Droughts	(-)	28.1	25.1	11%
Mean Duration	(days)	490.2	483.6	1%
Mean Deficit Volume	(mm)	4.4	6.8	-54%
Mean Intensity	(mm/day)	0.02	0.03	-40%
Mean St. Deficit Volume	(day)	15.5	21.0	-35%

The number of droughts times the mean duration is far higher than 20% of the time, what it should be according to the threshold method (see also Section 3.3.2). This is caused by the large differences in number of droughts and mean duration within climate E. There are cells with one drought of over 3000 days, and cells with 81 droughts with an average duration of 39 days. Because number of

droughts and mean duration vary over a different range (0-81 number of droughts and 39-3275 days duration respectively) the mean of both characteristics is not proportionate to each other anymore. Per individual cell it is still true that there is only drought 20% of the time. Appendix F.2 shows the relation between the mean duration and the number of droughts in each cell.

The E climates have on average the lowest number of droughts of all major climates. The radiation-based method and the temperature-based method came up with on average 28.1 and 25.1 droughts respectively in more than 40 years. As a consequence of the definition of drought, the mean duration of a drought event is long in comparison with the other climates due to the low number of droughts, both methods came up with a mean duration of more than 480 days per drought event. There are quite large discrepancies between the two methods for the drought characteristics, as shown in Table 18, compared to other climates but also compared to Appendix F.2. Yet the relative differences are still lower than the relative differences found between observed and modeled drought characteristics in Van Huijgevoort *et al.* (2011).

The two sub climates have quite a different behavior as well, see Appendix E.3. The differences between the two methods are much higher for the EF than for the ET sub climate.

4 Concluding remarks

There is a substantial difference in the reference evapotranspiration (ET_0) between the radiation-based and temperature-based methods. For all climates together the mean absolute difference is 31.1 mm/month. In more than 76% of the cases the radiation-based method leads to higher evapotranspiration than the temperature-based method. The climate with the largest differences in ET_0 is the arid B-climate, with a mean absolute difference of 48.5 mm/month. Not surprisingly, the climates with the lowest mean absolute difference are the colder D and the E climates with a mean absolute difference of 19.6 and 16.2 mm/month respectively, see Appendix F.1.

The evapotranspiration regimes (i.e. the mean monthly ET graphs) show that in all major climates the radiation-based method leads on average to a higher ET_0 than the temperature-based method, except for the hot arid climates, climate B.

For ET_A , the actual evapotranspiration, the differences between the two methods are substantially smaller. The mean absolute difference decreased to 11.4 mm/month (63% reduction). Interesting detail here is that the B-climate now has the smallest mean absolute difference; 3.1 mm/month (due to the absence of soil moisture, see Appendix F.1). In all climates, except A and C, the zero differences increased substantially from ET_0 to ET_A . For all climates, 26.4% of all differences equaled zero, for climate E this was even 62.8%.

In general (all climates together), ET_A radiation-based leads on the northern hemisphere to higher ET_A , on the southern hemisphere both methods alternate. The same holds for major climates C, D² and E. In climate A the radiation-based method on both hemispheres leads to higher actual evapotranspiration numbers, in climate B both methods alternate on both hemispheres.

There are considerable differences in drought characteristics because of the two different methods to compute reference evapotranspiration, but compared with other literature (e.g. Van Loon *et al.*, 2011, Van Huijgevoort *et al.*, 2011) the differences are in general within an acceptable range. For all climates together the differences in number of drought and average duration are only 3% and 8%, respectively. The volume-associated drought characteristics have larger differences (18-29%), but absolute numbers are rather small. For climates A and B the differences are small, all characteristics have less than 16% difference (difference for number and duration are less than 10%). For climates D and E on the other hand, the differences are much larger, up to 56% and 54% difference for the mean deficit volume respectively. Except for the number of droughts (which is negatively correlated with the mean duration), the temperature-based method leads to higher numbers for all characteristics; duration, deficit volume, intensity and standardized deficit volume. The largest relative disagreement exists in the mean deficit volume and the mean intensity, but absolute numbers are smallest.

Overall it can be concluded that the two different methods certainly lead to different results for ET_0 , ET_A and drought characteristics, but the differences are within a range that is found in literature. It is not possible to say if these differences occurred due to inconsistencies in the WFD, or due to the different calculation method that is used.

²Climate D has no cells in the southern hemisphere in the selected WFD

References

- Allen, R.G., Pereira, L.S. and Raes, D. (1998) *Crop Evapotranspiration: Guidelines for Computing Crop Water Requirements*, FAO Report no. 56, Rome, Italy.
- Changnon, S.A.Jr. (1987) *Detecting drought conditions in Illinois*, ISWS/CIR-169-87, 36 pp., Ill. State Water Surv., Champaign.
- Hisdal, H., Tallaksen, L.M., Clausen, B., Peters, E. and Gustard, A. (2004) *Hydrological Drought Characteristics*, pg. 139-198 in: *Hydrological Drought Processes and Estimation Methods for Streamflow and Groundwater* (L. M. Tallaksen and H. A. J. Van Lanen, eds), *Developments in Water Science*, 48, Elsevier The Netherlands.
- IPCC (2007) *Climate Change 2007: The Physical Science Basis. Contribution of Working Group I to the Fourth Assessment Report of the Intergovernmental Panel on Climate Change*, (Solomon, S., D. Qin, M. Manning, Z. Chen, M. Marquis, K.B. Averyt, M. Tignor and H.L. Miller, eds.). Cambridge University Press, Cambridge, United Kingdom and New York, NY, USA, 996 pp.
- Kotttek, M., Grieser, J., Beck, C., Rudolf, B. and Rubel, F. (2006) World Map of the Köppen-Geiger climate classification updated, *Meteorologische Zeitschrift*, **15**, 593-611, 657-679.
- Kraijenhoff van de Leur, D.A. (1958) A study of non-steady groundwater flow with special reference to a reservoir-coefficient, *De Ingenieur*, **19**, 87-94.
- Mishra A.K. and Singh, V.P. (2010) A review of drought concepts. *Journal of Hydrology*, **391**, 202-216.
- Mitchell, T.D. and Jones, P.D. (2005) An improved method of constructing a database of monthly climate observations and associated high-resolution grids, *International Journal of Climatology*, **25**, 693-712.
- Monteith, J.L. (1965) *Evaporation and environment*, pg. 205-234 in: *Symposium of the Society for Experimental Biology* (Fogg, G.E., eds), Vol. 19, Cambridge University Press, Cambridge, United Kingdom
- Ritzema, H.P. (1994) *Subsurface Flow to Drains*, pg. 263-303 in: *Drainage Principles and Applications*, 2nd edition, International Institute for Land Reclamation and Improvement (Ritzema, H.P, eds), Wageningen, The Netherlands.
- Schneider, U., Fuchs, T., Meyer-Christoffer, A. and Rudolf, B. (2008) *Global Precipitation Analysis Products of the GPCC.*, Global Precipitation Climatology Centre (GPCC). Deutscher Wetterdienst, Offenbach am Mainz, Germany (gpcc.dwd.de)
- Seibert, J. (2005) *HBV light version 2, user's manual*. Stockholm University, Department of Physical Geography and Quaternary Geology.
- Stull, R. (2000) *Meteorology for scientists and engineers, 2nd edition*, Brooks/Cole Thomson learning. pg 99.
- Tallaksen, L.M., and Van Lanen, H.A.J.(2004) *Hydrological drought: processes and estimation methods for streamflow and groundwater*, *Developments in Water Science* 48, Elsevier Science B.V.
- Tallaksen, L.M., Hisdal, H., and Van Lanen, H.A.J. (2009) Space-time modelling of catchment scale drought characteristics, *Journal of Hydrology*, **375**, 363-372.
- Uppala, S.M., Kallberg, P.W., Simmons, A.J., Andrae, U., Bechtold, V.D., Fiorino, M., Gibson, J.K., Haseler, J., Hernandez, A., Kelly, G.A., Li, X., Onogi, K., Saarinen, S., Sokka, N., Allan, R.P.,

Andersson, E., Arpe, K., Balmaseda, M.A., Beljaars, A.C.M., Van De Berg, L., Bidlot, J., Bormann, N., Caires, S., Chevallier, F., Dethof, A., Dragosavac, M., Fisher, M., Fuentes, M., Hagemann, S., Holm, E., Hoskins, B. J., Isaksen, I., Janssen, P., Jenne, R., McNally, A. P., Mahfouf, J. F., Morcrette, J.J., Rayner, N.A., Saunders, R.W., Simon, P., Sterl, A., Trenberth, K.E., Untch, A., Vasiljevic, D., Viterbo, P. and Woollen, J. (2005) The ERA-40 re-analysis. *Quarterly Journal of the Royal Meteorological Society*, **131**, 2961-3012.

Van Huijgevoort, M.H.J., Van Loon, A.F., Hanel, M., Haddeland, I., Horvát, O., Koutroulis, A., Machlica, A., Weedon, G., Fendeková, M., Tsanis, I., Van Lanen, H.A.J. (2011), *Simulation of low flows and drought events in WATCH test basins: impact of different climate forcing datasets*, WATCH Technical Report no. 26, 43 pg.

Van Lanen, H.A.J., Weerts, A.H., Kroon, T. and Dijkema, R. (1996) Estimation of groundwater recharge in areas with deep groundwater tables using transient groundwater flow modelling. *Proceedings of International Conference on 'Calibration and Reliability of Groundwater Modelling'*, September 1996, **Golden, USA**, pg. 307-316.

Van Lanen, H.A.J., Wanders, N., Tallaksen, L.M., and Van Loon, A.F. (2011) Hydrological drought across the world: relative impact of hydroclimatology and physical catchment structure, *Journal of Hydrometeorology* [submitted]

Van Loon, A.F., Van Lanen, H.A.J., Hirdal, H., Tallaksen, L.M., Fendeková, M., Oosterwijk, J., Horvát, O. and Machlica, A. (2010) *Understanding hydrological winter drought in Europe*. pg. 189-197 in: *Global Change: Facing Risks and Threats to Water Resources* (Servat, E., Demuth, S., Dezetter, A., Daniell, T., Ferrari, E., Ijjaali, M., Jabrane, R., Van Lanen, H. and Huang, Y., eds), IAHS Publ. No. 340

Van Loon, A.F., Van Lanen, H.A.J., Tallaksen, L.M., Hanel, M., Fendeková, M., Machlica, M., Sapriza, G., Koutroulis, A., Van Huijgevoort, M.H.J., van, Jódar Bermúdez, J., Hirdal, H. and Tsanis, I. (2011) *Propagation of drought through the hydrological cycle*. WATCH Technical Report No. 32, 97 pg.

Wanders, N., Van Lanen, H.A.J. and Van Loon, A.F. (2010) *Indicators for drought characterization on a global scale*. WATCH Technical Report No. 24, 54 pg. [available at: <http://www.eu-watch.org/publications/technical-reports/>].

Weedon, G.P., Gomes, S., Viterbo, P., Shuttleworth, W.J., Blyth, E., Österle, H., Adam, J.C., Belouin, N., Boucher, O., and Best, M. (2011) Creation of the WATCH Forcing Data and its use to assess global and regional reference crop evaporation over land during the twentieth century. *Journal of Hydrometeorology* [submitted]

Willhite, D.A. (ed.) (2000) *DROUGHT A Global Assessment, Vol I and II*, Routledge Hazards and Disasters Series, Routledge, London, UK.

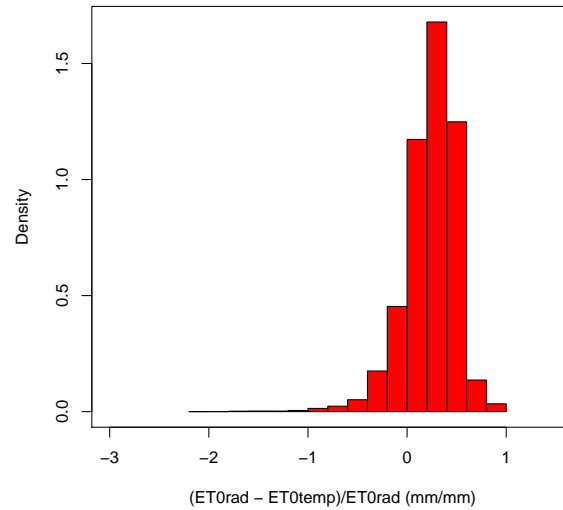
Wösten, J.H.M., Veerman, G.J., De Groot, W.J.M., and Stolte, J. (2001) *Waterretentie,- en doorlatendheidskarakteristieken van boven,- en ondergronden in Nederland: de Staringreeks.*, Technical Report no. 153, Alterra, Wageningen [available at: <http://www2.alterra.wur.nl/Webdocs/PDFFiles/Alterraraapporten/AlterraRapport153.pdf>].

WWDR (2009) World Water Assessment Programme 2009. The United Nations World Water Development Report 3: Water in a Changing World. Paris: UNESCO, and London: Earthscan.

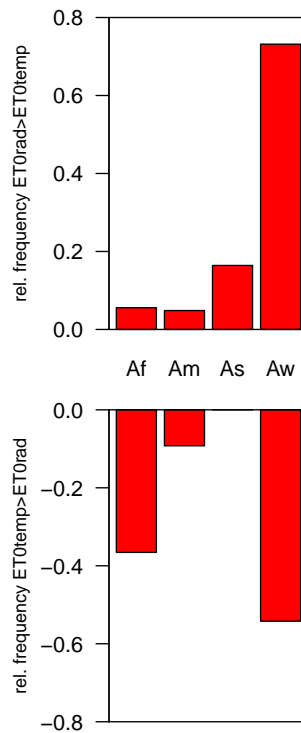
Appendices

A Climate A

A.1 Reference evapotranspiration ET_0

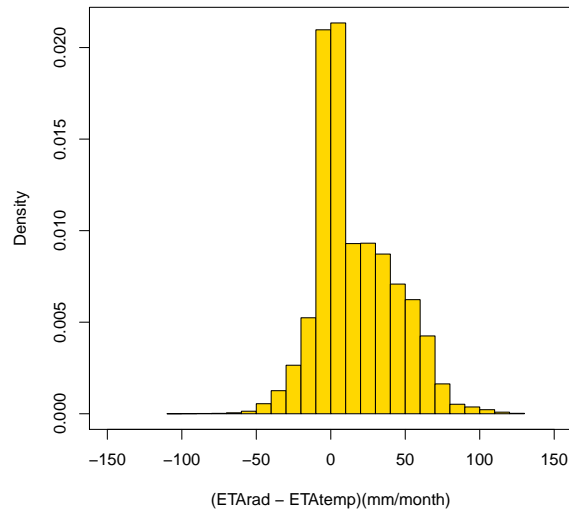


St.Differences in ET_0 between radiation-based and temperature-based methods for climate A.

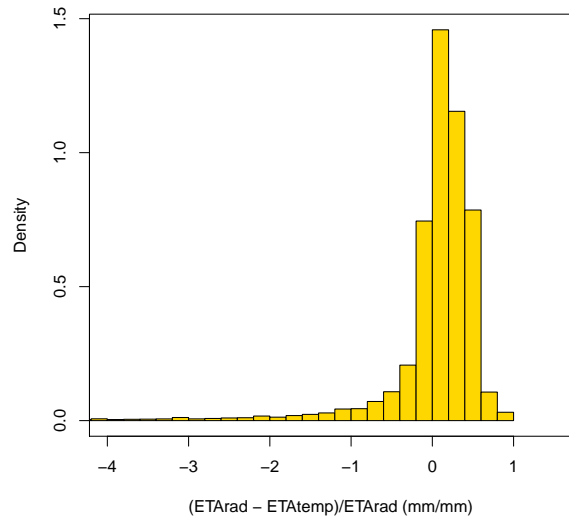


Relative frequency of A sub climates in highest 1% differences. In the upper graph radiation-based ET_0 is higher than temperature-based ET_0 , in the lower graph temperature-based ET_0 is higher.

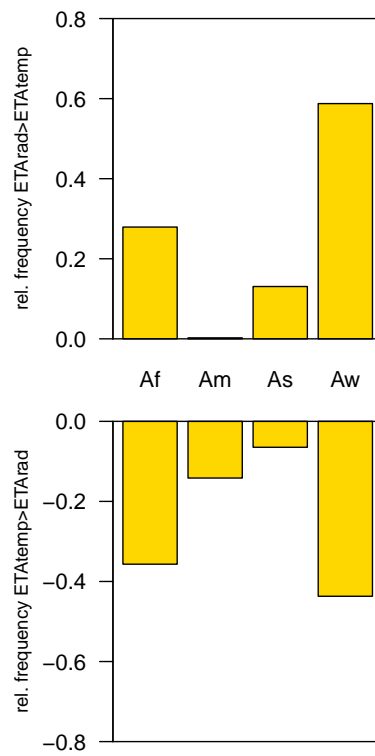
A.2 Actual evapotranspiration ET_A



Differences in ET_A between radiation-based and temperature-based method for climate A.



St.Differences in ET_A between radiation-based and temperature-based method for climate A.



Relative frequency of A sub climates in highest 1% differences. In the upper graph radiation-based ET_A is higher than temperature-based ET_A , in the lower graph temperature-based ET_A is higher.

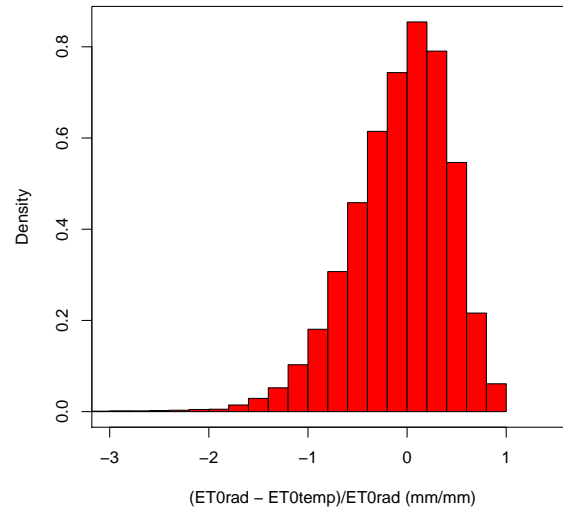
A.3 Hydrological drought characteristics

Drought characteristics per sub climate within major climate A, and difference relative to radiation-based method in percentage

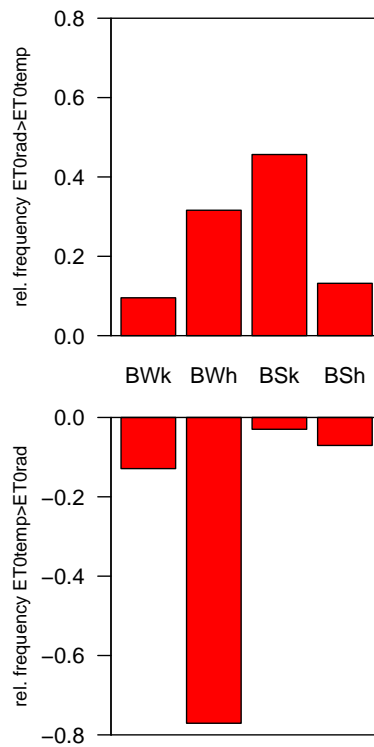
		nr.of droughts	mean duration	mean def.volume	mean intensity	mean st.def.volume
Af	rad.	66.6	63.9	29.0	0.12	6.9
	temp.	58.2	60.2	29.9	0.13	6.2
	diff.	12.6	5.9	-3.2	-6.1	10.3
Am	rad.	58.5	61.7	21.3	0.09	6.5
	temp.	53.3	66.2	25.5	0.1	6.7
	diff.	9.0	-7.3	-19.3	-16.2	-3.6
As	rad.	53.9	64.5	9.4	0.05	7.0
	temp.	51.7	68.2	11.4	0.06	7.6
	diff.	4.0	-5.8	-20.3	-21.2	-8.8
Aw	rad.	62.6	55.2	8.7	0.05	5.4
	temp.	61.1	56.7	10.9	0.06	5.7
	diff.	2.5	-2.8	-25.7	-24.3	-4.4

B Climate B

B.1 Reference evapotranspiration ET_0

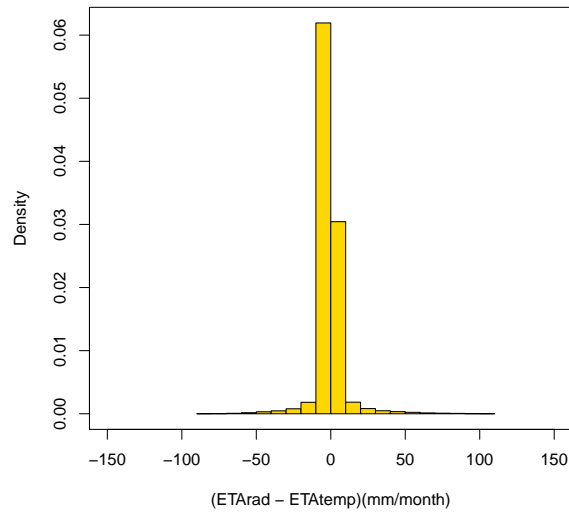


St.Differences in ET_0 between radiation-based and temperature-based method for climate B.

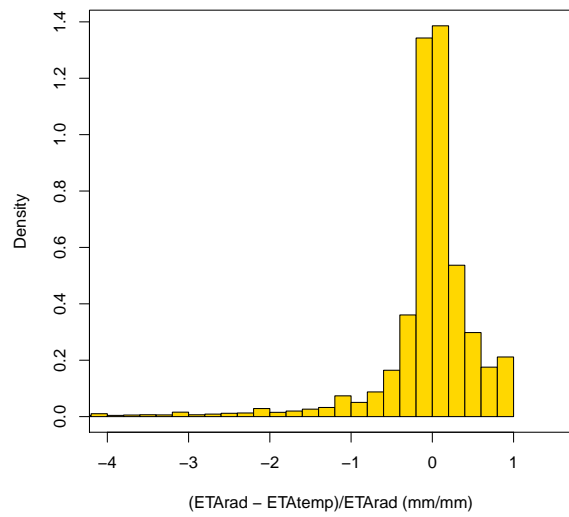


Relative frequency of B sub climates in highest 1% differences. In the upper graph radiation-based ET_0 is higher than temperature-based ET_0 , in the lower graph temperature-based ET_0 is higher.

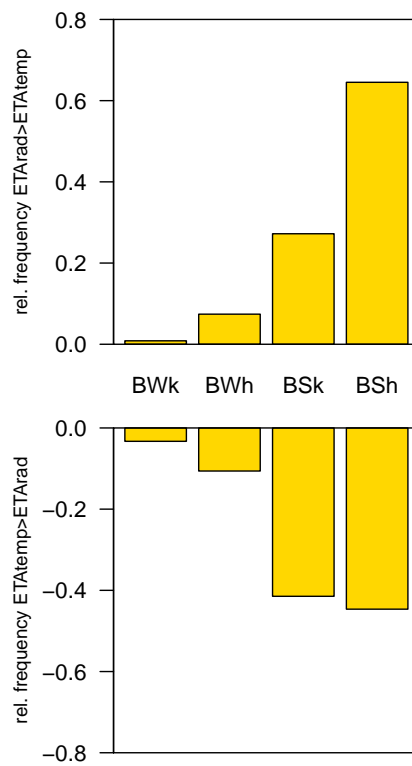
B.2 Actual evapotranspiration ET_A



Differences in ET_A between radiation-based and temperature-based method for climate B.

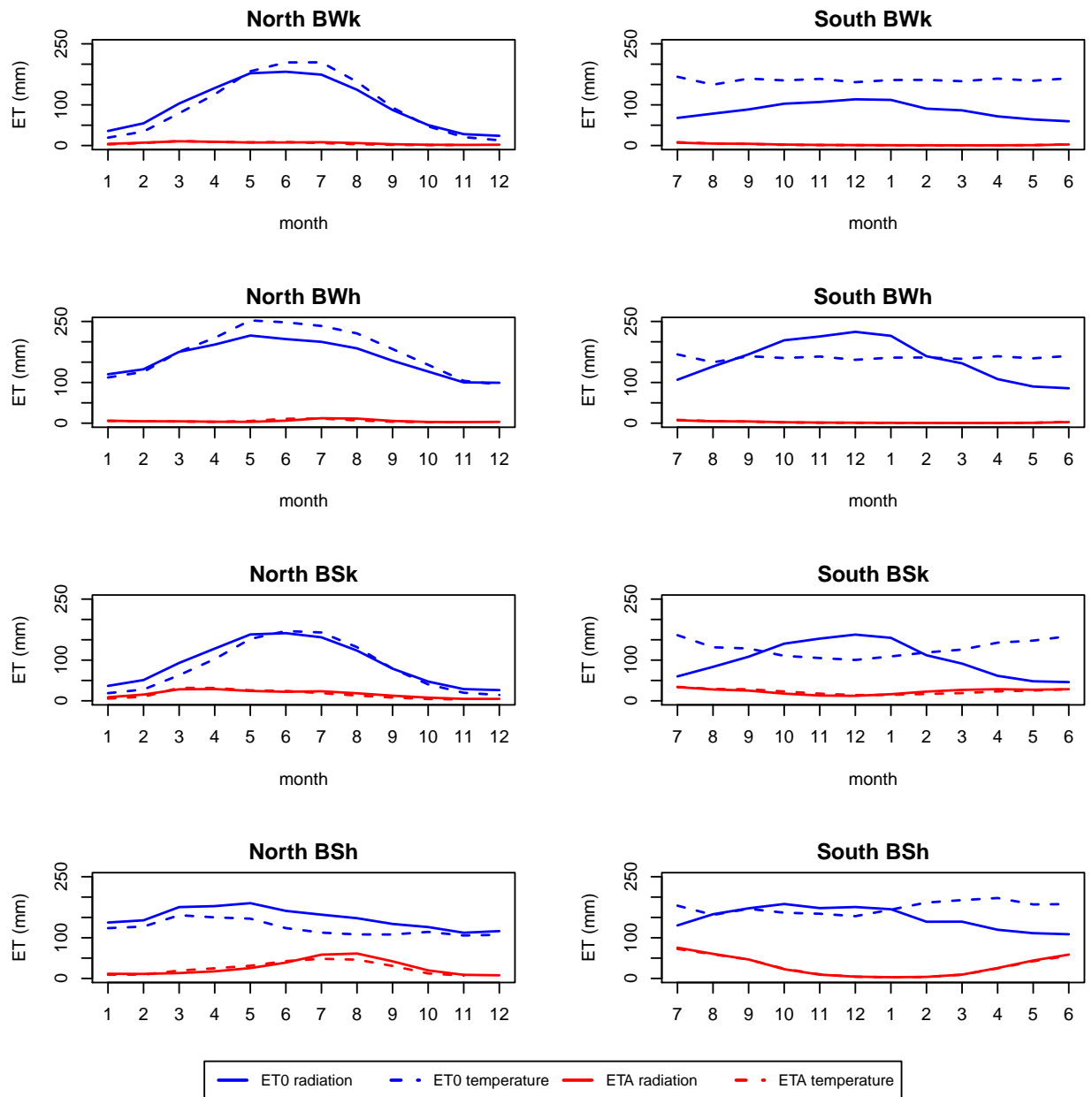


St.Differences in ET_A between radiation-based and temperature-based method for climate B.



Relative frequency of B sub climates in highest 1% differences. In the upper graph radiation-based ET_A is higher than temperature-based ET_A , in the lower graph temperature-based ET_A is higher.

B.2 Actual evapotranspiration ET_A



ET_0 and ET_A throughout the year for the sub climates of major climate B, divided over the northern and southern hemisphere. Note difference in x-axis.

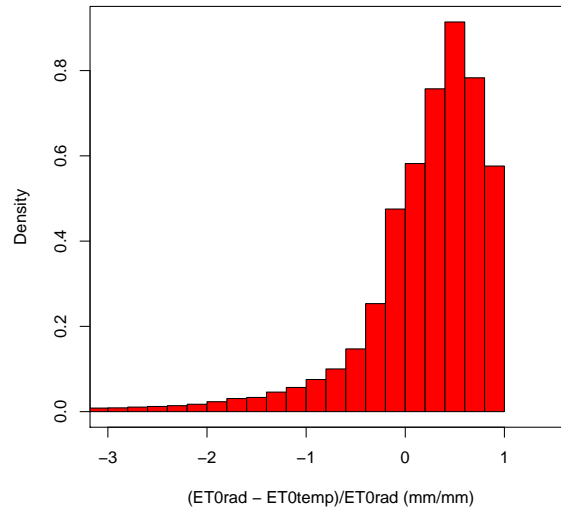
B.3 Hydrological drought characteristics

Drought characteristics per sub climate within major climate B, and difference relative to radiation-based method in percentage

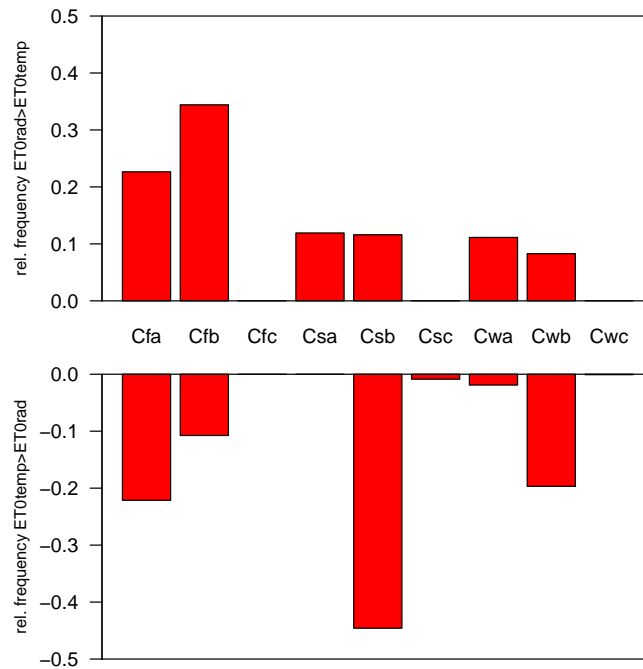
	nr.of droughts	mean duration	mean def.volume	mean intensity	mean st.def.volume
BWk rad.	32.4	205.4	0.8	0.004	15.2
temp.	32.8	204.8	0.8	0.004	15.1
diff.	-1.2	0.3	2.0	2.8	0.6
BWh rad.	20.7	618.2	2.0	0.008	15.7
temp.	20.9	621.3	2.0	0.007	15.5
diff.	-1.1	-0.5	0.8	0.6	0.9
Bsk rad.	59.6	59.3	1.8	0.011	6.9
temp.	57.3	63.9	1.9	0.012	7.5
diff.	3.8	-7.7	-9.7	-2.8	-8.6
BSh rad.	53.5	63.0	3.6	0.021	7.1
temp.	50.7	67.6	4.5	0.023	7.7
diff.	5.0	-7.3	-26.4	-10.6	-9.8

C Climate C

C.1 Reference evapotranspiration ET_0

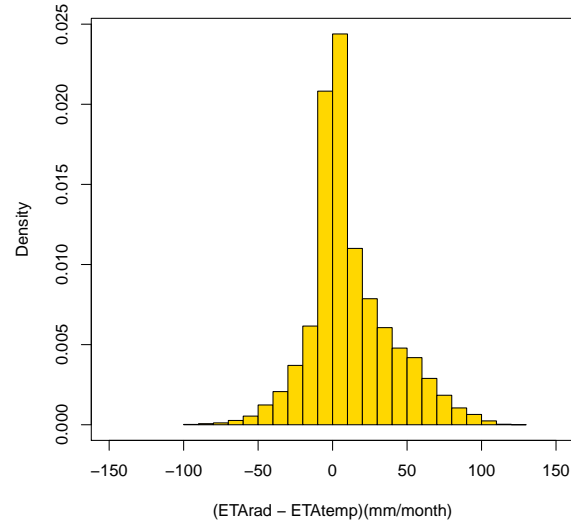


St.Differences in ET_0 between radiation-based and temperature-based method for climate C.

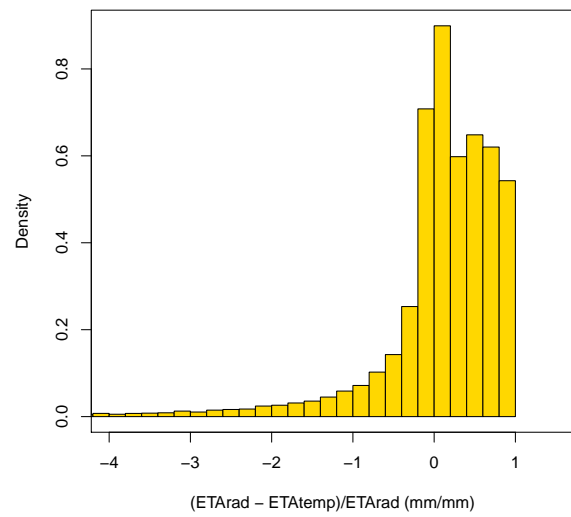


Relative frequency of C sub climates in highest 1% differences. In the upper graph radiation-based ET_0 is higher than temperature-based ET_0 , in the lower graph temperature-based ET_0 is higher.

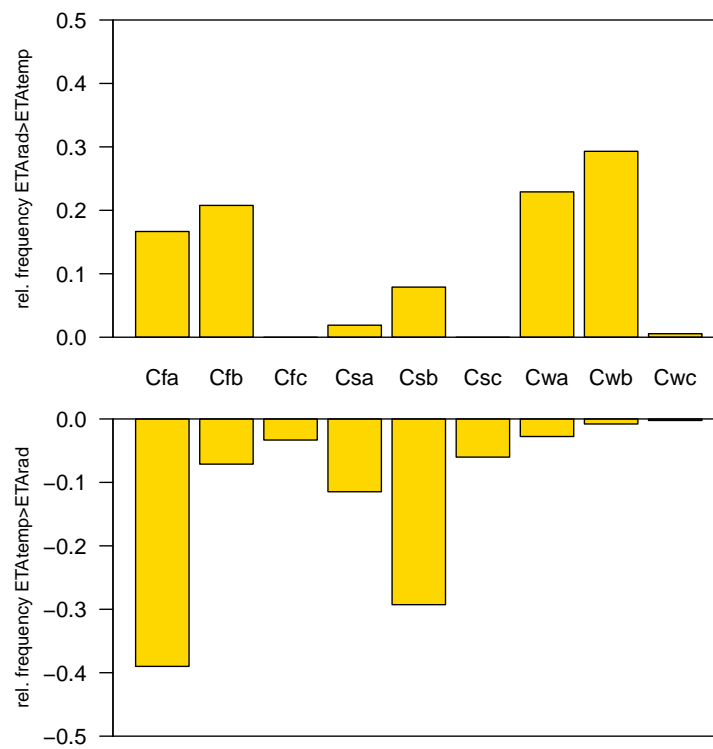
C.2 Actual evapotranspiration ET_A



Differences in ET_A between radiation-based and temperature-based method for climate C.



St.Differences in ET_A between radiation-based and temperature-based method for climate C.



Relative frequency of C sub climates in highest 1% differences. In the upper graph radiation-based ET_A is higher than temperature-based ET_A , in the lower graph temperature-based ET_A is higher.

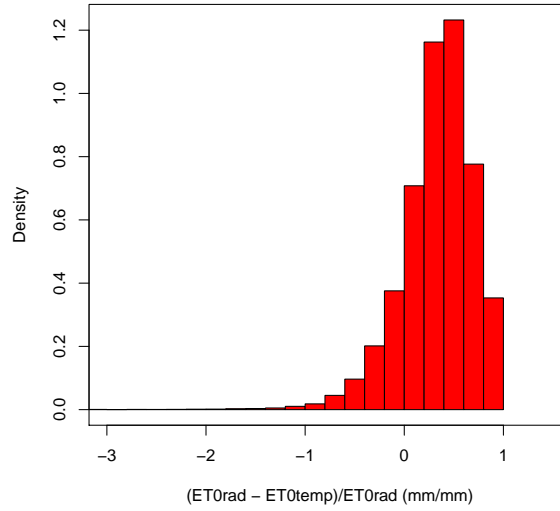
C.3 Hydrological drought characteristics

Drought characteristics per sub climate within major climate C, and difference relative to radiation-based method in percentage

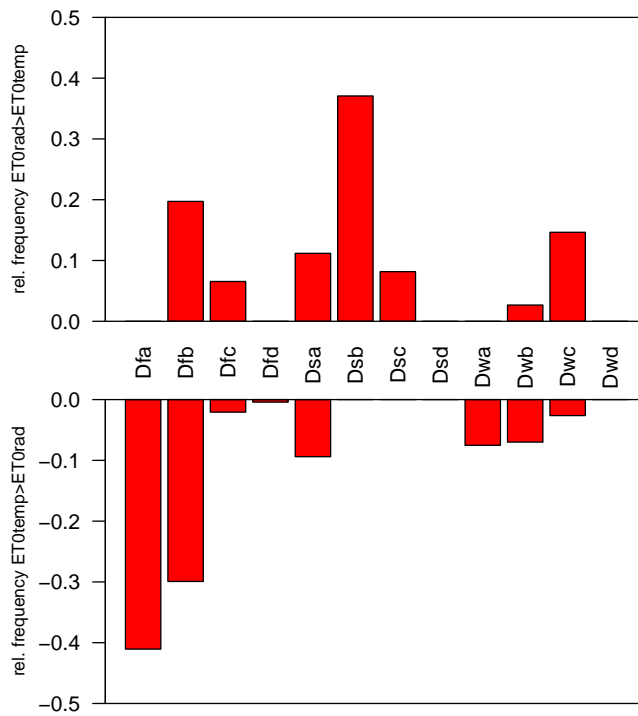
		nr.of droughts	mean duration	mean def.volume	mean intensity	mean st.def.volume
Cfa	rad.	70.9	48.6	8.0	0.048	4.5
	temp.	68.0	51.9	9.3	0.056	4.9
	diff.	4.2	-6.9	-17.3	-15.7	-8.2
Cfb	rad.	58.9	60.1	7.6	0.042	6.2
	temp.	57.8	63.5	10.4	0.057	4.9
	diff.	1.9	-5.8	-36.5	-35.2	-6.6
Cfc	rad.	68.0	55.0	10.2	0.062	5.8
	temp.	79.6	46.2	9.6	0.065	4.3
	diff.	-17.1	16.0	6.0	-4.9	25.6
Csa	rad.	57.2	60.0	6.2	0.032	6.5
	temp.	43.0	84.2	10.1	0.047	10.0
	diff.	24.8	-40.4	-62.3	-45.4	-54.5
Csb	rad.	58.9	57.8	9.4	0.048	6.4
	temp.	59.6	64.0	9.9	0.054	6.6
	diff.	-1.3	-10.6	-5.4	-10.5	-2.9
Csc	rad.	57.8	59.3	6.4	0.026	6.9
	temp.	73.4	51.4	3.8	0.023	5.3
	diff.	-26.9	13.3	40.8	13.9	22.6
Cwa	rad.	59.0	59.3	11.0	0.052	6.5
	temp.	54.0	64.4	14.2	0.064	6.5
	diff.	8.4	-8.5	-28.6	-23.3	-1.1
Cwb	rad.	70.3	47.7	5.6	0.046	3.9
	temp.	66.3	55.0	8.9	0.061	5.2
	diff.	5.6	-15.2	-57.8	-33.3	-31.1
Cwc	rad.	60.3	56.6	4.4	0.030	5.6
	temp.	54.2	64.8	7.1	0.039	7.6
	diff.	10.1	-14.6	-61.1	-27.6	-35.5

D Climate D

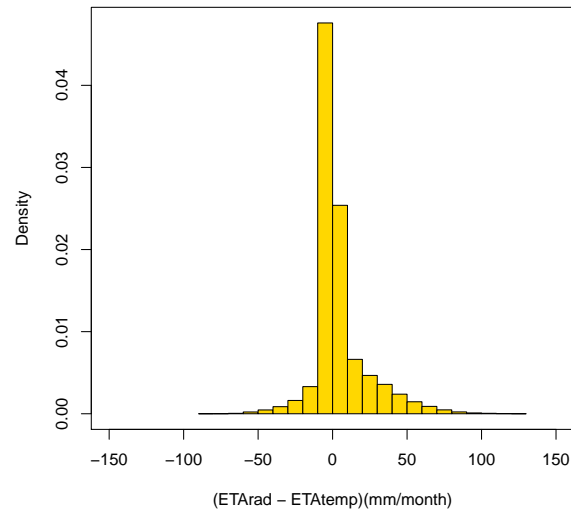
D.1 Reference evapotranspiration ET_0



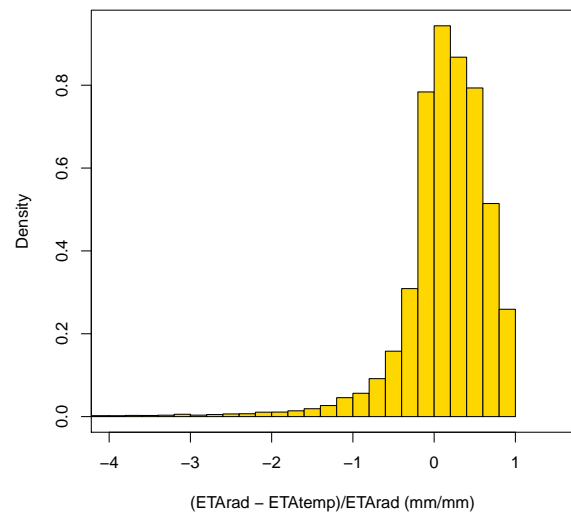
St. Differences in ET_0 between radiation-based and temperature-based methods in mm/mm for climate D.



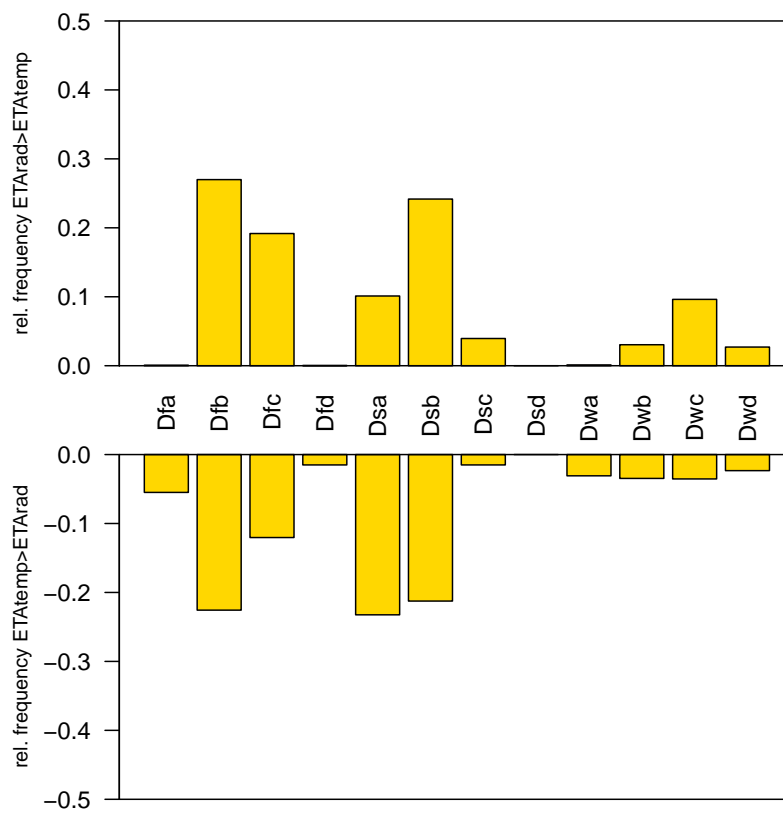
Relative frequency of D sub climates in highest 1% differences. In the upper graph radiation-based ET_0 is higher than temperature-based ET_0 , in the lower graph temperature-based ET_0 is higher.

D.2 Actual evapotranspiration ET_A 

Differences in ET_A between radiation-based and temperature-based method for climate D.



St.Differences in ET_A between radiation-based and temperature-based method for climate D.



Relative frequency of D sub climates in highest 1% differences. In the upper graph radiation-based ET_A is higher than temperature-based ET_A , in the lower graph temperature-based ET_A is higher.

D.3 Hydrological drought characteristics

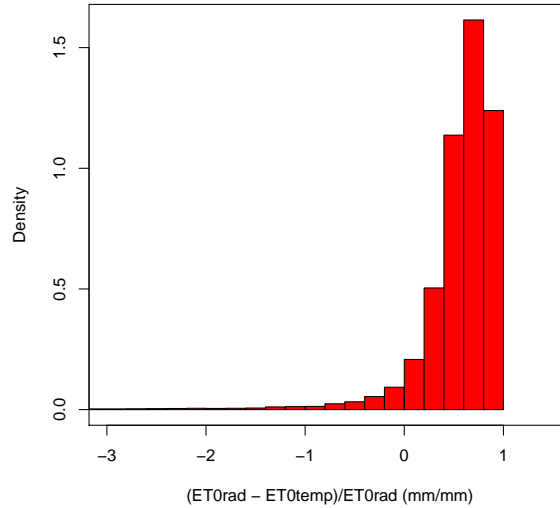
Drought characteristics per sub climate within major climate D, and difference relative to radiation-based method in percentage

		nr.of droughts	mean duration	mean def.volume	mean intensity	mean st.def.volume
Dfa	rad.	65.9	51.7	2.3	0.017	5.6
	temp.	64.9	51.9	2.5	0.017	5.7
	diff.	1.5	-0.5	-11.5	-5.3	-2.2
Dfb	rad.	60.5	55.4	4.2	0.029	5.3
	temp.	55.5	62.9	6.2	0.039	6.4
	diff.	8.3	-13.5	-47.2	-34.5	-20.0
Dfc	rad.	51.2	68.3	4.7	0.030	7.2
	temp.	44.8	78.0	6.8	0.040	8.7
	diff.	12.4	-14.1	-46.5	-34.0	-20.7
Dfd	rad.	54.5	60.9	1.3	0.011	6.3
	temp.	38.0	106.0	3.8	0.015	13.7
	diff.	30.3	-74.1	-188.0	-42.6	-117.2
Dsa	rad.	56.5	60.1	3.0	0.020	6.1
	temp.	43.4	83.5	5.7	0.027	10.4
	diff.	23.1	-39.0	-90.0	-39.0	-70.0
Dsb	rad.	48.8	68.8	5.0	0.027	7.8
	temp.	42.6	76.1	7.5	0.040	9.1
	diff.	12.7	-10.6	-50.2	-51.0	-16.2
Dsc	rad.	55.5	62.7	2.2	0.013	7.0
	temp.	36.7	97.7	4.9	0.020	12.6
	diff.	33.8	-55.7	-123.0	-53.4	-78.7
Dsd ¹						
Dwa	rad.	74.6	43.6	2.5	0.018	3.5
	temp.	69.7	49.1	3.8	0.024	4.3
	diff.	6.5	-12.6	-56.1	-27.6	-24.9
Dwb	rad.	65.6	52.4	2.7	0.017	4.9
	temp.	51.8	66.4	4.6	0.026	6.4
	diff.	21.0	-26.7	-71.4	-49.7	-31.1
Dwc	rad.	61.9	55.2	2.4	0.016	5.2
	temp.	52.0	66.1	4.0	0.024	6.5
	diff.	16.1	-19.8	-65.8	-50.1	-26.0
Dwd	rad.	58.5	56.8	1.3	0.010	5.4
	temp.	30.8	111.6	4.2	0.022	12.6
	diff.	47.4	-96.3	-225.4	-122.5	-133.8

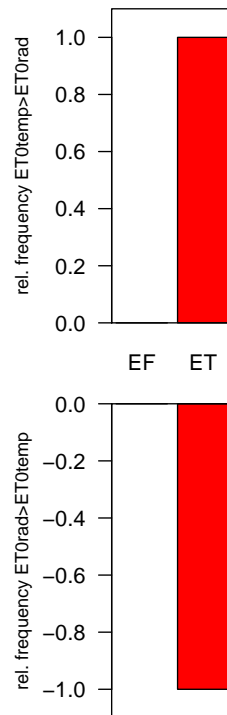
¹This climate does not exist within the WFD

E Climate E

E.1 Reference evapotranspiration ET_0

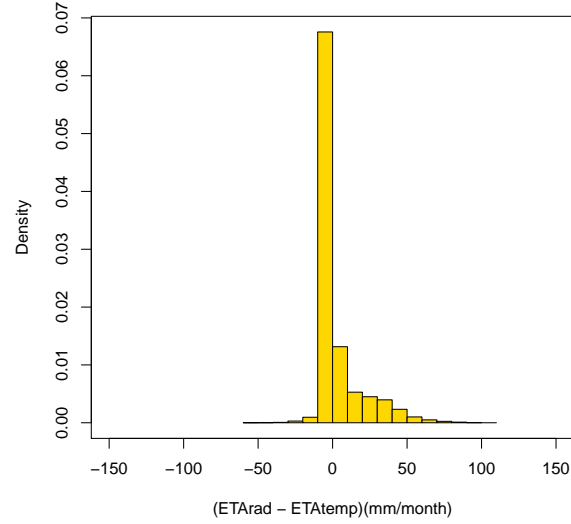


St.Differences in ET_0 between radiation-based and temperature-based method for climate E.

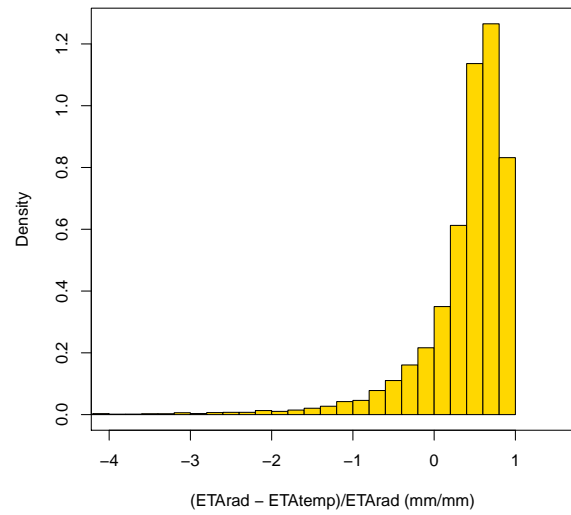


Relative frequency of E sub climates in highest 1% differences. In the upper graph radiation-based ET_0 is higher than temperature-based ET_0 , in the lower graph temperature-based ET_0 is higher.

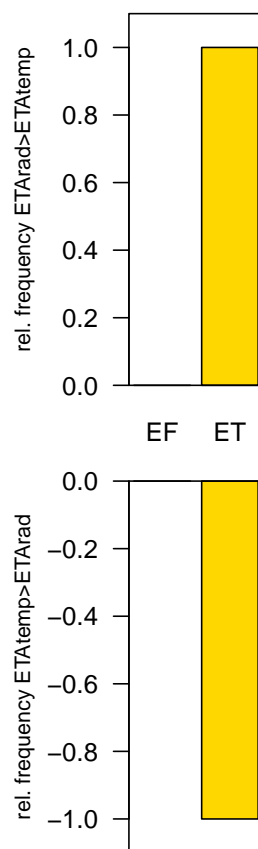
E.2 Actual evapotranspiration ET_A



Differences in ET_A between radiation-based and temperature-based method for climate E.



St.Differences in ET_A between radiation-based and temperature-based method for climate E.



Relative frequency of E sub climates in highest 1% differences. In the upper graph radiation-based ET_A is higher than temperature-based ET_A , in the lower graph temperature-based ET_A is higher.

E.3 Hydrological drought characteristics

Drought characteristics per sub climate within major climate E, and difference relative to radiation-based method in percentage

		nr.of droughts	mean duration	mean def.volume	mean intensity	mean st.def.volume
EF	rad.	4.7	1990.9	0.4	0.001	19.5
	temp.	3.6	1865.1	1.2	0.001	32.3
	diff.	23.9	6.3	-228.3	-138.6	-66.1
ET	rad.	33.9	112.7	5.4	0.024	14.6
	temp.	30.5	136.1	8.2	0.034	18.1
	diff.	10.3	-20.8	-51.1	-39.4	-24.3

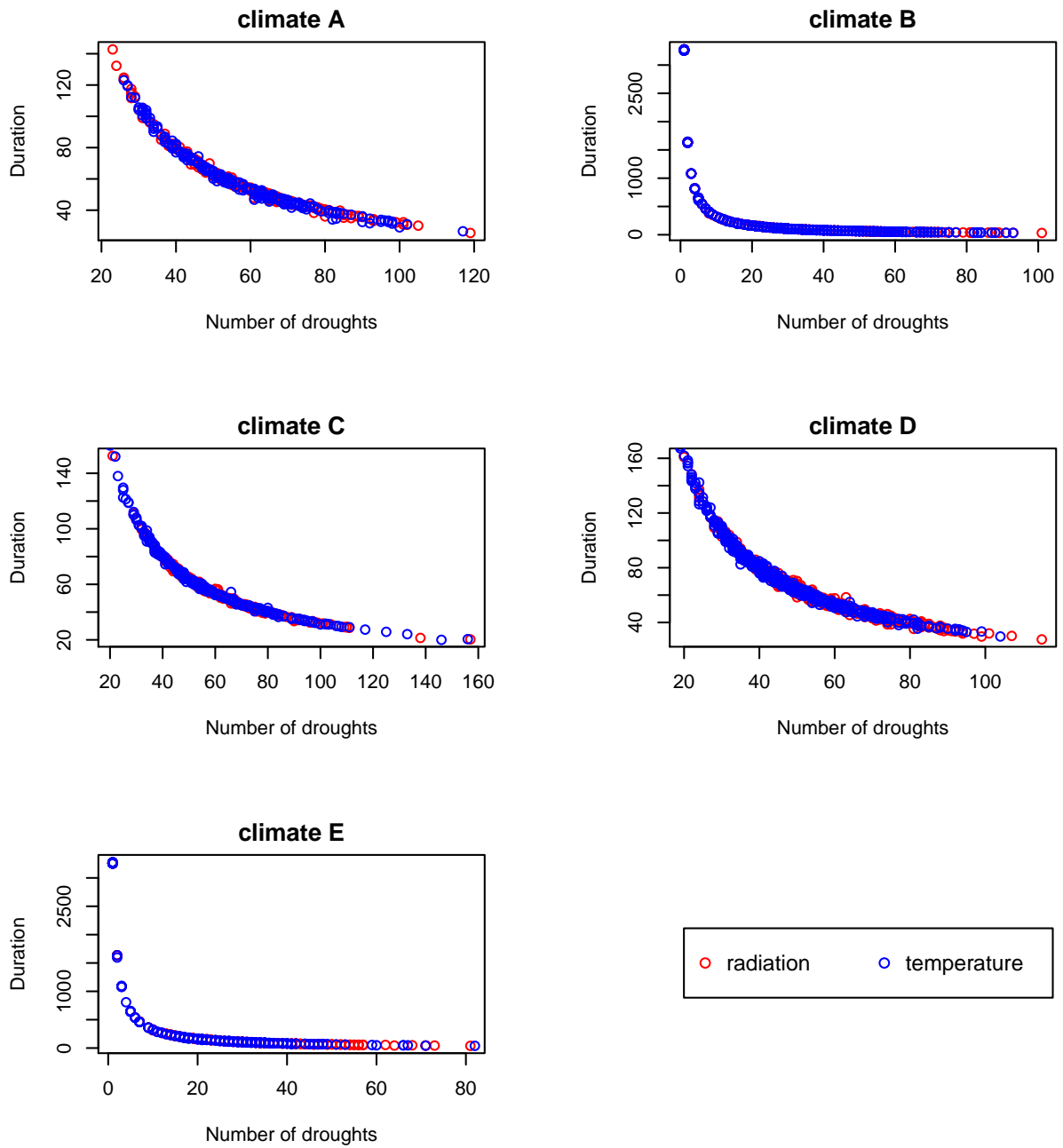
F Overview

F.1 Evapotranspiration ET

Overview of ET_0 and ET_A numbers mentioned in chapter 3

Climate	Mean diff.	Abs.diff.	% Diff 20.0mm	% Diff 20.0mm	Min.diff.	Max.diff.	% ET_{rad} ET_{temp}	% ET_{temp} ET_{rad}	> 0%	% St.Diff 0.25mm
<i>ET₀</i>										
All	11.6	31.1	46.2	-336.2	142.4	76.4	23.3	0.3	29.9	
A	30.6	37.6	25.4	-133.9	129.0	85.4	14.6	0.1	42.3	
B	-15.5	48.5	30.3	-336.2	142.4	49.3	50.6	0.1	39.5	
C	18.6	38.7	30.9	-182.2	138.9	72.7	27.7	0.1	26.0	
D	15.1	19.6	64.4	-244.8	131.4	84.1	15.3	0.6	28.4	
E	14.3	16.2	68.6	-76.4	119.6	93.8	5.9	0.3	8.4	
<i>ET_A</i>										
All	7.1	11.4	78.8	-105.3	129.0	48.3	25.3	26.4	58.7	
A	16.4	22.0	56.9	-105.3	129.0	69.1	29.3	1.6	52.3	
B	0.2	3.1	96.0	-80.3	108.8	34.4	33.2	32.4	72.3	
C	11.7	20.4	62.4	-96.9	123.0	65.0	33.5	1.5	37.6	
D	5.3	9.3	82.9	-83.5	127.5	45.9	22.3	31.9	59.5	
E	5.6	6.3	87.0	-58.8	100.1	31.1	6.1	62.8	68.2	

F.2 Hydrological drought characteristics



The average duration of a drought event versus the number of droughts per cell per major climate. Note the differences in X and Y-axis.

Differences in drought characteristics between two different forcing sets (local and WFD). The difference is given in percentage and defined relative to the WFD numbers. Adapted from Van Huijgevoort *et al.* (2011)

Catchment	Model	Dataset	Number of droughts	Duration of drought	Deficit drought
Narsjø (Norway)	HBV-WUR	Local	128.0	25.8	5.3
	HBV-WUR	WFD	128.0	23.8	5.5
	Difference		0	-8.6	3.3
	HBV-NVE	Local	221.0	13.4	3.2
	HBV-NVE	WFD	157.0	19.7	3.8
	Difference		-40.8	31.7	16.9
Upper-Metuje (Czech Republic)	HBV-WUR	Local	69.0	21.2	1.2
	HBV-WUR	WFD	82.0	18.0	0.9
	Difference		15.9	-17.7	-34.5
	BILAN	Local	46.0	32.3	3.0
	BILAN	WFD	48.0	31.5	2.9
	Difference		4.2	-2.5	-0.7
Upper-Sázava (Czech Republic)	HBV-WUR	Local	124.0	21.6	1.2
	HBV-WUR	WFD	111.0	25.1	1.8
	Difference		-11.7	14.1	35.3
	BILAN	Local	67.0	42.5	3.4
	BILAN	WFD	66.0	44.7	3.4
	Difference		-1.5	4.9	-2.1
Nedožery (Slovakia)	HBV-WUR	Local	103.0	19.2	1.8
	HBV-WUR	WFD	102.0	18.4	1.4
	Difference		-1.0	-4.0	-27.3
	BILAN	Local	39.0	37.2	3.0
	BILAN	WFD	48.0	30.2	2.5
	Difference		18.8	-23.4	-21.2
Platis (Crete)	HBV-TUC	Local	69.0	30.4	3.9
	HBV-TUC	WFD	81.0	24.9	2.8
	Difference		14.8	-22.1	-37.5